AN EXPERIMENTAL PARAMETERIZATION FOR SENSIBLE HEAT FLUX AND COMPUTATION OF SURFACE AIR TEMPERATURE FOR VARIOUS DESERT AREAS

by

STARLEY L. THOMPSON

Department of Meteorology
Texas A & M University
College Station, Texas 77843

12 May 1976

ABSTRACT

The energy flux terms in the surface heat balance equation were computed using parameterizations and mean monthly temperature, precipitation, planetary albedo, cloudiness, and vapor pressure data for 85 very dry locations. The major flux terms, solar radiation absorbed (S), net longware radiation (I), and sensible heat flux (H), for January and July are presented for 60 stations in North Africa. Sensible heat exchange between the air and surface was then parameterized by a regression procedure using the mean monthly values computed as residuals in the heat balance equation. H was found to be a function of S and the proximity of the station to a major water body (D). Larger H surface losses occur for larger values of S and/or smaller values of D. The regression equation for H explains 96% of the variance of the original computations. Knowing approximate expressions for all the terms in the heat balance equation, mean monthly surface air temperature was computed to test the efficacy of the H parameterization. The computed temperatures (T_c) show a combination of systematic and random deviations from the observed temperatures to the extent that the average root-mean-square error of T_c for all stations is 10°C. Thus, the derived expression for H has limited computational usefulness. Improvements in the parameterization could perhaps be made by replacing constants with simple functions or by dividing the stations into two or more geographical regions for separate study.

1. Introduction

Knowledge of Earth's surface temperature is necessary for the full understanding of energy exchanges that occur between the atmosphere and the surface. Conversely, it is possible, through suitable parameterization of the surface energy fluxes in the basic heat balance equation, to arrive at a value of surface temperature (Saltzman, 1967). Recent meteorological research has sought to provide such a method of computing surface temperature adequate for use as a lower boundary condition in models simulating the general circulation of the atmosphere (Bhumralker, 1975; Vernekar, 1975). General circulation models generate temperatures and wind velocities at specific levels in the atmosphere; these elements are, in turn, used as input to various surface energy flux expressions, specifically those for exchange of sensible and latent heat between the atmosphere and the surface.

Surface temperature may also be determined as an end product in simpler surface climate models, such as the ones developed by Myrup (1969) and Outcalt (1972). These models also require explicit knowledge of wind speed and temperature advection for the computation of surface sensible heat flux.

It should be possible to replace knowledge of the atmospheric circulation in certain climatic regimes with other meteorological and/or geographical information to arrive at a new parameterization for sensible heat exchange. The purpose of the present study is to determine a suitable method for computing mean monthly surface air (screen height) temperatures for selected desert areas without explicit knowledge of the general circulation patterns affecting those areas. To

accomplish this, values of sensible heat flux, computed as residuals in the heat balance equation, will be parameterized by statistical regression procedures for a number of desert areas. This new expression will then be inserted in the heat balance equation, and mean monthly surface temperatures for the desert stations will be computed to test the efficacy of the parameterization.

2. The heat balance equation

For an infinitesimally thin layer at the air-soil interface the heat fluxes across the interface must be continuous. Thus, the heat balance equation is

$$S + I + H + LE + G = 0$$

Here S is the absorbed flux of solar radiation at the interface; H, LE, and I are, respectively, the sensible and latent heat fluxes and net longwave radiation all immediately above the interface, and G is the heat flux immediately below the interface (soil heat flux). Positive and negative values denote fluxes directed toward, and away, from the interface. Here fluxes are considered to be time rates of energy per unit area.

To simplify the solution of (1) very dry areas have been chosen for study. In such areas the radiation and sensible heat terms greatly dominate the surface heat balance, and the LE term is comparatively small. The magnitude of G is always relatively small at any land location; the maximum values hardly ever exceed 10% of the net radiation (S+I) (Sellers, 1965).

The instantaneous flux of solar radiation absorbed by a horizontal surface can be written

$$J = (1-\alpha) \left(\frac{r_m}{r}\right)^2 S_o T^m \cos\theta \qquad (2)$$

Here r_m and r are the mean Earth-Sun distance and the instantaneous Earth-Sun distance, respectively; S_o is the solar constant; T is the gross zenith transmissivity of the atmosphere, empirically derived; m, the optical air mass; θ, the zenith angle of the sun; and α the planetary albedo at the location in question. The gross zenith path transmissivity (direct plus diffuse radiation) is inversely related to the precipitable water in a clear atmosphere.[1] For most of the stations in this study the mean monthly precipitable water varies from 1.25cm to 1.9cm (Tuller, 1968). A constant value of T equal to 0.85, corresponding to 1.5cm of precipitable water, was determined from data in Smithsonian Meteorological Tables (1966). The solar constant was assumed to be 1353 W m^{-2} (1.94 ly min^{-1}). The optical air mass was approximated by

$$m = \sec\theta$$

The mean monthly value of solar radiation absorbed can be determined by integrating (2) from sunrise to sunset and then summing the daily values for an entire month so that

$$S = \frac{1}{\Delta t} \sum_{i=1}^{N} \int_{t_{ri}}^{t_{si}} J \, dt \qquad (3)$$

where Δt is the length of the month; N is the number of days in the

month; and t_{si} and t_{ri} are time of sunset and sunrise on the i th day of the month, respectively. The exact procedure for computing S is explained in the Appendix.

The form of the parameterization for net longwave radiation is taken from Budyko (1974).

$$I = -d\sigma T^4(1-\beta n^{\gamma})(a-be^{\frac{1}{2}}) \tag{4}$$

Here σ is the Stefan-Boltzman constant; T is the soil surface temperature; n is the fraction of the sky covered by clouds; e is the vapor pressure in millibars; and d, β, γ, a, and b are empirical constants. Values for d, β, and γ are from Budyko (1974). The coefficient β is a function of latitude because it is assumed the mean frequency of different cloud types varies approximately with latitude (Berliand and Berliand, 1952). A constant value of β corresponding to a latitude of 18 N or S, the approximate mean latitude of the desert areas in this study, was used. The empirical constants a and b are median values derived from several researchers as suggested by Sellers (1965). The constant values used in (4) are:

$$\begin{aligned} d &= 0.95 \\ \sigma &= 5.67 \times 10^{-8} \text{ W m}^{-2} \text{ K}^{-4} \\ \beta &= 0.58 \\ \gamma &= 1.5 \\ a &= 0.395 \\ b &= 0.048 \text{ mb}^{-\frac{1}{2}} \end{aligned}$$

An expression for heat flux into the soil was taken from the work of Bhumralker (1975). He derives the following:

$$G_z = -(\frac{\omega c \lambda}{2})^{\frac{1}{2}}(\frac{1}{\omega}\frac{\partial T_z}{\partial t} + T_z - \overline{T}) \tag{5}$$

Here G_z is the heat flux into the soil at an arbitrary depth z; ω is the angular frequency of oscillation of the annual surface temperature wave; c is the volumetric heat capacity of the soil; λ is the thermal

conductivity; T_z is the soil temperature at depth z; and $\overline{T}$ is the temperature of the soil at a depth of negligible annual temperature variation. By applying (5) at the surface we get,

$$G = -c_1 \frac{\partial T}{\partial t} - c_2 (T - \overline{T}), \tag{6}$$

where $c_1 = (\frac{c\lambda}{2\omega})^{\frac{1}{2}}$,

and $c_2 = (\frac{\lambda c \omega}{2})^{\frac{1}{2}}$.

From (6) it can be seen that the greatest heat flux into the soil (-G) occurs when the surface temperature is high compared to the mean soil temperature and when the surface temperature is increasing most rapidly. This agrees with observations (Sellers, 1965) showing that heat flux into the soil reaches a maximum in late spring, not during midsummer as would be expected if the time rate of temperature change had no effect.

Thermal conductivity and volumetric heat capacity, which are functions of soil material and moisture content, were assumed to be constant for the desert areas considered. Values taken from Priestly (1959) corresponding to two-thirds dry sand and one-third organic soil were used. The constant values in (6) are as follows:

$$c = 1.63 \times 10^6 \text{ J m}^{-3} \text{ K}^{-1}$$
$$\lambda = 0.51 \text{ J m}^{-1} \text{ K}^{-1} \text{ sec}^{-1}$$
$$\omega = 1.991 \times 10^{-7} \text{ sec}^{-1}$$

The parameterization for latent heat flux simply assumes that all the precipitation that falls is immediately evaporated, thus

$$LE = -LP_m,$$

where L is the latent heat of evaporation and P_m is the mass of the precipitation per unit area per unit time. For L taken as a constant

equal to 2.45×10^6 J kg^{-1}, and converting P_m to an equivalent depth of precipitation, we have

$$LE = -0.932P \text{ W } m^{-2} \text{ mm}^{-1} \tag{7}$$

where P is the mean monthly precipitation in millimeters.

If S, I, G, and LE are computed by the use of (3), (4), (6), and (7), the exchange of sensible heat may be determined as the residual term in (1).

Equations (4) and (6) require knowledge of the soil surface temperature. In most cases this information is difficult to obtain and must be approximated. The simplest way to approximate the soil surface temperature is to assume that the ratio of the mean annual range of the soil surface temperature to the mean annual range of the air temperature is a known constant. According to de Vries (1958), this ratio is generally between 1.1 and 2. For simplicity the ratio was assumed to be unity in this study, i.e., the mean monthly soil surface temperature was set equal to the mean monthly air temperature. Such an assumption may result in an error in the mean annual range of net longwave radiation because of its strong dependence on temperature. The concomitant error in the mean annual range of sensible heat flux should alter the constants in an eventual parameterization slightly, but the form of the expression will remain unchanged.

3. Data and derived quantities

Meteorological data for this study comprised mean monthly values of surface air temperature, precipitation, cloud amount, planetary albedo ($\bar{\alpha}$), and vapor pressure for each desert station. Selection criteria required that each station have less than 50 millimeters of

mean annual precipitation, and all climatic means had to be based on a record of at least five years duration. In all, data from 85 stations in Africa, South America, the Middle East, and the United States were used. Geographical data consisted of the latitude, elevation and distance from a major water body for each station. Major water bodies considered in this study were the Mediterranean Sea, the Atlantic and Pacific Oceans, and the Red Sea.

Temperature, precipitation, and geographical information were taken from World Weather Records, 1951-60 (U. S. Department of Commerce, 1967, 1966), Strahler (1965), Rumney (1968), Wernstedt (1961a, b), and World Survey of Climatology (Griffiths, 1972). Distance data were taken from maps in the Hammond Medallion World Atlas (1971).

Mean monthly cloud amount for January and July was taken from Schutz and Gates (1973, 1974). Missing values were substituted for from Schutz and Gates (1971, 1972b). January and July vapor pressures for Africa and Israel are from World Survey of Climatology (Griffiths, 1972). Vapor pressures for South America and Saudi Arabia were calculated using temperature and relative humidity data from Schutz and Gates (1971, 1972b). Values of e for Greenland Ranch, California were derived from dewpoint information in World Survey of Climatology (Bryson, 1974).

Values of January planetary albedo were taken from Schutz and Gates (1972a) for South America and southern Africa, and from Schutz and Gates (1973) for the rest of the stations. July planetary albedo data for all stations but those in South America and southern Africa are from Schutz and Gates (1974). For the remaining stations $\overline{\alpha}$ was

computed as an average of the planetary albedos of Schutz and Gates (1974) and albedos estimated by the author based on mean monthly cloud amount and surface albedo. This was done because the tabulated $\bar{\alpha}$ values alone appeared to be too small. Albedo due to clouds was calculated using the expression suggested by Berliand (1960):

$$\alpha_c = (g + hn)n$$

where g = 0.38 and h is a function of latitude. For this study, the variation of latitude was small and h was held constant at a representative value of 0.38. Surface albedo values were taken from Schutz and Gates (1972b). Surface albedos (α_s) and cloud albedos (α_c) were combined using the expression

$$\alpha_e = \alpha_c + \alpha_s - \alpha_c \alpha_s$$

to give an estimated planetary albedo (α_e).

Values of e, n, and $\bar{\alpha}$ for the entire year were derived by linear interpolation between January and July.

Eq. (6) requires $\frac{\partial T}{\partial t}$ and $\bar{T}$ to be derived from temperature data before G can be determined. The time derivative of T was computed by a centered finite difference formula:

$$\frac{\partial T}{\partial t} = (T_{+1} - T_{-1})/2\Delta t$$

where T_{-1} is the previous month's temperature, T_{+1} is the next month's temperature, and Δt is the average length of a month. The arithmetic mean of the mean monthly temperatures were taken as $\bar{T}$.

4. Flux computation results

Surface heat fluxes for each station-month were computed using the expressions in Section 2. Figures 2 through 7 show the distribu-

tion of the major components of the surface energy balance for North Africa for the months of January and July. The maps were drawn from computations for 60 stations. The distribution of the stations is shown in Fig. 1. The remaining 25 stations were too widely scattered for an efficient map presentation of the heat flux results.

Figs. 2 and 3 show the mean solar radiation absorbed by the surface for January and July. In January, the amount absorbed increases southward and is almost exclusively a function of latitude. The gradient is reversed in July with high values of S to the north. In general, the January and July results show good agreement with the maps of Schutz and Gates (1971, 1972b, after Budyko, 1963), and with the results of Vernekar (1975). The values presented by the former source are for solar radiation received at the surface; they were modified for comparison with Figs. 2 and 3 by taking into account the surface albedo. The July values of S for the west coast of North Africa are high as compared to Schutz and Gates (1972b), but agree well with Vernekar (1975).

Mean net long wave radiation (I) for January and July is shown in Figs. 4 and 5. The fields are similar for the two months, and a maximum occurs in southern Algeria, where -I is over 100 W m^{-2} in January and 120 W m^{-2} in July. Low magnitudes of I are associated with areas of relatively high vapor pressure near major water bodies. Again these values are in good agreement with those of Schutz and Gates (1971) and Vernekar (1975) for January, but appear to be low as compared to Schutz and Gates (1972b) for July.

The computed mean flux of sensible heat for January and July is

shown in Figs. 6 and 7. January values follow latitude lines with larger magnitudes toward the summer hemisphere. The July field has a pronounced minimum in Algeria (where -I is large) and high values of sensible heat loss in coastal areas. These large negative values near large water bodies are presumably a consequence of the advection of cool air over the land surface which, in turn, enhances heat loss due to turbulence and small scale convection. January values show good agreement with Schutz and Gates (1971) and Vernekar (1975), but July values are too large. The difference with respect to Schutz and Gates (1972b) is due to the mismatch in net longwave radiation mentioned previously. The H values of Vernekar (1975) for July may be too small in magnitude due to his apparent overestimate of LE in North Africa.

Values of LE and G, not shown here, are generally an order of magnitude smaller than the major flux terms. Heat flux into the soil has a mean annual range of about 8 W m^{-2}; this is in good agreement with Sellers (1965).

Figures 8, 9, and 10 show the mean annual variation of the components of the surface heat balance and air temperature for three of the stations in the study. Antofagasta (Fig. 10) is a coastal station, while Aoulef (Fig. 8) and Faya-Largeau (Fig. 9) are both at interior locations. The three graphs are very similar. Each shows little annual variation of I; higher e values in summer tend to offset higher temperatures. Sensible heat loss follows the S curve closely. Heat flux into the soil is negligible for Antofagasta due to the small mean annual temperature range.

5. A regression formula for H

All the heat fluxes in (1) except sensible heat exchange were computed using known approximate relations or parameterizations. Sensible heat flux (H) was thus determined as the residual in this expression. But, as was noted in the introduction, surface temperature is the desired element, and it would be of greater utility to know H and treat temperature as the unknown. Since the remaining terms of (1) appear to be highly correlated with H, a regression procedure is suggested, and an attempt will now be made to find an empirical expression that will give H as a function of more easily obtained quantities.

A multiple linear regression procedure was used. The dependent data set comprised the 1020 mean monthly values of H computed for the desert stations. The predictor or independent variables chosen were air temperature, solar radiation absorbed, ln(D+10) where D is the distance from the nearest major water body in kilometers, elevation, and various non-linear combinations of the preceding variables. A regression procedure was chosen that produced the "best" one variable model, "best" two variable model, etc., by maximizing the square of the correlation coefficient, R. Only two variables, S and ln(D+10), made significant contributions to R^2. The resulting regression expression for sensible heat flux is:

$$H_r = k_1 + k_2 S + k_3 \ln(D+10), \tag{8}$$

where $k_1 = 37.3$

$k_2 = -0.951$

$k_3 = 7.69$

The units of H_r are W m^{-2}. Thus the sensible heat loss ($-H_r$) from a desert surface is proportional to solar radiation absorbed and greater for small values of D. The dependence of H on D is largely due to the effect of cool air advection near the coasts of large bodies of water. Eq. (8) explains 96% of the variance of the original H data.

The mean fields of regression sensible heat flux computed from (8) for North Africa for January and July are shown in Fig. 11 and 12, respectively. The January values of H_r agree fairly well with those in Fig. 6 in magnitude and in location. The gradients of H_r are slightly greater than those of H along the west coast of North Africa. The isopleths of H_r also deviate northward over the Red Sea as a result of the D term in (8), whereas the field of H in Fig. 6 has no such distortion. The July values of H_r in Fig. 11 also are in fair agreement with those of H in Fig. 7. The major difference in the two maps is the absence of a center of minimum magnitude for H_r. The magnitude and geographical distribution agree well otherwise.

6. Computation of surface air temperature

With an explicit expression for each term in (1), mean monthly surface temperatures can be solved for as an unknown, thus testing the efficacy of (8) as a parameterization for sensible heat exchange in deserts.

Several modifications have to be made in the flux terms to facilitate the solution procedure. Eq. (6) contains a time derivative of T which, of course, makes (1) a differential equation. This derivative can be approximated by the simple two-point backward difference equation

$$\frac{\partial T}{\partial t} \simeq \frac{T - T_{-1}}{\Delta t} , \tag{9}$$

where T_{-1} is the previous month's temperature, and Δt is the length of the month. The mean annual temperature, $\overline{T}$, must also be known in (6) before values of T can be computed. Eq. (1) can be written as

$$\frac{1}{12} \left(\sum_i S_i + \sum_i LE_i + \sum_i G_i + \sum_i H_{ri} + \sum_i I_i\right) = 0 \tag{10}$$

where the summations are over the 12 months of the year. Denoting the mean annual values by a bar and recognizing that $\overline{G} = 0$, (1) becomes

$$\overline{S} + \overline{LE} + \overline{H}_r + \frac{1}{12} \sum_i I_i = 0$$

If the mean annual range of temperature is small compared to $\overline{T}$, we may make the approximation that

$$\frac{1}{12} \sum_i T_i^4 \simeq \left(\frac{1}{12} \sum_i T_i\right)^4 = \overline{T}^4$$

By substituting for I from (4) an expression for $\overline{T}$ is derived:

$$\overline{T} = \left[(\overline{S} + \overline{LE} + \overline{H}_r)/d\sigma(1-\beta n^{\gamma})(a-be^{\frac{1}{2}})\right]^{\frac{1}{4}} \tag{11}$$

The inclusion of (4) in (1) makes the resulting heat balance equation quartic in T. Although there are simple iterative techniques available for the solution of such a non-linear equation (see, e.g., Jacobs and Brown, 1973), it was decided to make a quadratic approximation to (4) as an optimum compromise between accuracy and rapid solubility. Making use of a Taylor series approximation centered on 293K, (4) becomes

$$I = d\sigma(1-\beta n^{\gamma})(a-be^{\frac{1}{2}})(q_1 + q_2 T + q_3 T^2) \tag{12}$$

Here $q_1 = -2.211 \times 10^{10}\ K^4$

$q_2 = 2.012 \times 10^{8}\ K^3$

$q_3 = -5.151 \times 10^{5}\ K^2$

Eq. (12) has an error of no more than 0.1%, as compared with (4), for the meteorological range of temperature in this study.

Eq. (1) can now be written as a combination of (6), (9), and (12), with S, H_r, LE, and $\overline{T}$ computed separately:

$$S + H_r + LE + d\sigma(1-\beta n^{\gamma})(a-be^{\frac{1}{2}})(q_1 + q_2T + q_3T^2) - c_1(T - T_{-1})/t - c_2(T - \overline{T}) = 0$$

This equation can be solved by use of the quadratic formula.

$$T_c = -[\mu_2 + (\mu_2^2 - 4q_3\mu_3)^{\frac{1}{2}}]/2q_3, \tag{13}$$

where T_c is the computed temperature,

$$\mu_2 = q_2 - (c_1/\Delta t + c_2)/\mu_4 \tag{14}$$

$$\mu_3 = q_1 + (S + H_r + LE + c_1 T_{-1}/\Delta t + c_2 \overline{T})/\mu_4 \tag{15}$$

$$\mu_4 = d\sigma(1-\beta n^{\gamma})(a - be^{\frac{1}{2}})$$

The previous month's temperature must be known in order to compute the temperature for any given month. For the initial month's computation no previous temperatures are known. However, mean monthly values of G for February are always relatively small. By making $c_1 = c_2 = 0$ for February (i.e., zero heat capacity and zero conductivity), G is forced to be zero. The inclusion of zero values of c_1 and c_2 in (14) and (15) allow T_c for February to be calculated. March, April, etc., temperatures are then computed using the true values of c_1 and c_2.

7. Results

Figures 13 and 14 show, respectively, the observed and computed mean surface air temperatures for northern Africa for January. The fields do not agree well, the major difference being the consistent

underestimate of the temperature in near-coastal areas. Indeed, the Red Sea has a warming influence in the observed field, but a pronounced minimum appears in that region in the T_c field. This is caused by H_r losses that are too large.

Observed and computed July mean temperatures are shown in Figs. 15 and 16. There is good agreement along the Atlantic and Mediterranean coasts. The mid-Sahara T maximum that is observed in Fig. 15 is replaced by a minimum in the T_c field. Again, temperatures near the Red Sea are underestimated, although this body of water does have a cooling effect in summer.

For the entire set of 85 stations there is a root-mean-square (RMS) error of H_r of 10.5 W m^{-2} as compared with the actual values of H. The corresponding RMS error of mean monthly computed temperatures is 10.6 K.

Figures 17-19 show the actual and computed annual variations of temperature and sensible heat for three different locations. Aoulef, Algeria (Fig. 17), is an example of good agreement between observed and computed temperatures. In Fig. 18 (Copiapo, Chile) the ranges of observed and computed temperatures do not agree. As can be seen, whenever H_r is lower than H, T_c is higher than T, and vice versa. The lower range of H_r as compared to H results in a higher range of T_c as compared to T. Fig. 19 shows computed temperatures for Casa Grande, Peru that are about 30°C higher than those observed. This error occurs because the magnitude of H_r is always smaller than that of H.

There are several sources for the error in the regression equation for H_r, and the concomitant error in computed temperature. Range

error such as that shown in Fig. 18 can be due to a non-constant value of k_2 in (8). Figure 20 shows actual H values plotted against absorbed solar radiation for three different stations. Although the correlation is linear, each line has a different slope. Values of this slope for the 85 stations vary from -0.8 to -1.1, with the more negative values in coastal areas, generally. The greater range of H for a given range of S in coastal areas is presumably due to high values of e and a corresponding low range of I. The constant value of k_2 of 0.951 overlooks this variation.

The water proximity term in (8) also is a source of error. Although $k_3 \ln(D+10)$ adds 6% to the 90% of the variance accounted for by solar radiation alone, there are definite problems associated with its inclusion. The term treats all water bodies equally. The coastal deserts of South America and western Africa are all influenced by cold currents and upwelling. Clearly, the Red Sea does not have the same effect that such currents have on coastal climate. The seasonal influence of large bodies of water is also neglected. Cold ocean currents may provide cool onshore advection all year. Smaller seas, such as the Red Sea, have a cooling influence in summer and a warming influence in winter (compare Figs. 13 and 15). Of course, the direction and strength of the prevailing winds serves to complicate the matter further. The constant, k_3, averages out all these differences with the result that no particular area receives proper treatment.

It is also possible that systematic errors in S, I, LE, or G could cause an otherwise perfect regression form for H to give erroneous results. This is probably a minor source of inaccuracy.

Figure 21 shows a scatter diagram of the RMS error of computed temperatures versus the RMS error of H_r for each station in the study. A proportional relationship exists between the two variables. From (1) and (4) we get

$$S + H + LE + G - d\sigma T^4(1-\beta n^\gamma)(a-be^{\frac{1}{2}}) = 0$$

It follows that

$$\frac{\partial T}{\partial H} = T^{-3}/4d\sigma(1-\beta n^\gamma)(a-be^{\frac{1}{2}}). \qquad (16)$$

By inserting the mean values of each of T, n, and e for all stations into (16) a slope is derived for a hypothetical "mean station":

$$\frac{\partial T}{\partial H} = 0.91°C\ W^{-1}\ m^2 \qquad (17)$$

A line with this slope is drawn in Fig. 21. This line fits the data points reasonably well. It should be noted that this is not the best fitting line in a statistical sense; it is instead a representative line, one of a family that can be derived from (16).

From (17) one can see that an error of only 1 W m^{-2} in H (or any other flux) results in about a 1°C error in temperature. This temperature departure is small on an absolute scale, but much larger considering the limited temperature range of meteorological interest. Thus, the terms in the heat balance equation need to be specified very accurately.

8. Conclusion

In an effort to develop a method of computing mean monthly surface air temperatures for deserts a parameterization for sensible heat exchange was developed for inclusion in the heat balance equation. A statistically valid expression for H was found, but systematic

errors combined with an overall lack of sufficient accuracy resulted in a formulation of limited computational usefulness.

It should be possible to improve the accuracy of the expression for H_r by making the regression coefficients in (8) simple functions. For example, k_2 appears to be correlated with D, and k_3 is not the same for all large water bodies. This would reduce some systematic error.

Breaking the current group of desert stations into two or more populations for study is an alternative method of improving the accuracy of H_r. For example, all deserts on the west coasts of continents could be considered as a separate group. But any improvement in H_r gained is paid for by a sacrifice of generality.

Of course, in the end, there is a limit to the accuracy one can achieve with a simple representation of a complex physical process like sensible heat exchange. Yet, such simple descriptions serve a useful purpose if they can aid in the understanding of the gross features of the heat balance at Earth's surface.

Acknowledgments. The initial impetus for this research resulted from the author's participation in the University Undergraduate Fellows Program of Texas A&M. I would like to extend my appreciation to Dr. D. M. Driscoll for his guidance during the research and preparation phases of the work. Also, I am grateful to Dr. G. A. Franceschini for his helpful comments on the manuscript. The author also thanks Mrs. Debbie Wisdom for typing the manuscript.

FOOTNOTE

[1]Eq. (2) is technically incorrect as stated. The combined use of α and T results in a double depletion from backscattering due to air, water vapor, and dust. However, dust depletion has been omitted from (2). The resulting equation therefore contains canceling errors and allows the use of planetary albedos, obtainable by satellite measurement.

Houghton (1954) adopted a dust transmission of 0.95^m. A mean value of the dust transmission can be obtained if a mean value of m is known. The optical air mass can be approximated by

$$\begin{aligned} m &= \sec\theta \\ &= (\cos\theta)^{-1} \\ &= (\sin\phi \sin\delta - \cos\phi \cos\delta \cos t)^{-1}, \end{aligned}$$

where ϕ is latitude, δ is the solar declination, and t is the solar hour angle (t = 0 at midnight). The mean optical air mass is

$$\bar{m} = [(\phi_2 - \phi_1)(\delta_2 - \delta_1)(t_2 - t_1)]^{-1} \int_{\phi_1}^{\phi_2} \int_{\delta_1}^{\delta_2} \int_{h_1}^{h_2} m \, dh \, d\delta \, d\phi$$

For the stations in this study the latitude limits are roughly $\phi_2 = 30°$, $\phi_1 = 5°$. The solar declination ranges from $\delta_2 = 23.5°$ to $\delta_1 = -23.5°$ during the year. The hour angle at noon is $h_1 = 0°$, and h_2 is the hour angle at sunrise. As a result of the integration, $\bar{m}$ is approximately 2. Thus, on the average, about 9% of the solar radiation reaching the lower troposphere is depleted by dust. Barry and Chorley (1970) show that, on the average, 6% of the solar radiation incident at the top of the atmosphere is scattered outward by air, dust, and water vapor (greater than 6% if one considers a percentage

based on the solar radiation reaching the lower troposphere). Since dust depletion and depletion due to backscattering are approximately equal, it is justifiable to include planetary albedo and omit dust depletion in (2).

FIGURE LEGENDS

Fig. 1. Location of stations in North Africa.

Fig. 2. Mean solar radiation absorbed (W m^{-2}) for January.

Fig. 3. Mean solar radiation absorbed (W m^{-2}) for July.

Fig. 4. Mean net longwave radiation (W m^{-2}) for January.

Fig. 5. Mean net longwave radiation (W m^{-2}) for July.

Fig. 6. Mean sensible heat flux (W m^{-2}) for January.

Fig. 7. Mean sensible heat flux (W m^{-2}) for July.

Fig. 8. Average annual variation of the air temperature and components of the surface energy balance at Aoulef, Algeria (26.97N). LE is negligible.

Fig. 9. Average annual variation of the air temperature and components of the surface energy balance at Faya-Largeau, Chad (18.00N).

Fig. 10. Average annual variation of the air temperature and components of the surface energy balance at Antofagasta, Chile (23.47S). LE and G are negligible.

Fig. 11. Mean regression sensible heat flux (W m^{-2}) for January.

Fig. 12. Mean regression sensible heat flux (W m^{-2}) for July.

Fig. 13. Observed mean surface air temperature (°C) for January.

Fig. 14. Computed mean surface air temperature (°C) for January.

Fig. 15. Observed mean surface air temperature (°C) for July.

Fig. 16. Computed mean surface air temperature (°C) for July.

Fig. 17. Annual variation of observed temperature (T), sensible heat flux (H), computed temperature (T_c), and regression sensible heat flux (H_r) for El Golea, Algeria (30.57N).

Fig. 18. Annual variation of observed temperature (T), sensible heat flux (H), computed temperature (T_c), and regression sensible heat flux (H_r) for Copiapo, Chile (27.35S).

Fig. 19. Annual variation of observed temperature (T), sensible heat flux (H), computed temperature (T_C), and regression sensible heat flux (H_r) for Casa Grande, Peru (7.68S).

Fig. 20. Sensible heat flux as a function of solar radiation absorbed for three locations. A. Luderitz Bay, Namibia (26.63S). B. Tor, Egypt (28.23N). C. Greenland Ranch, California, United States (36.47N).

Fig. 21. RMS error of computed temperature as a function of RMS error of regression sensible heat flux.

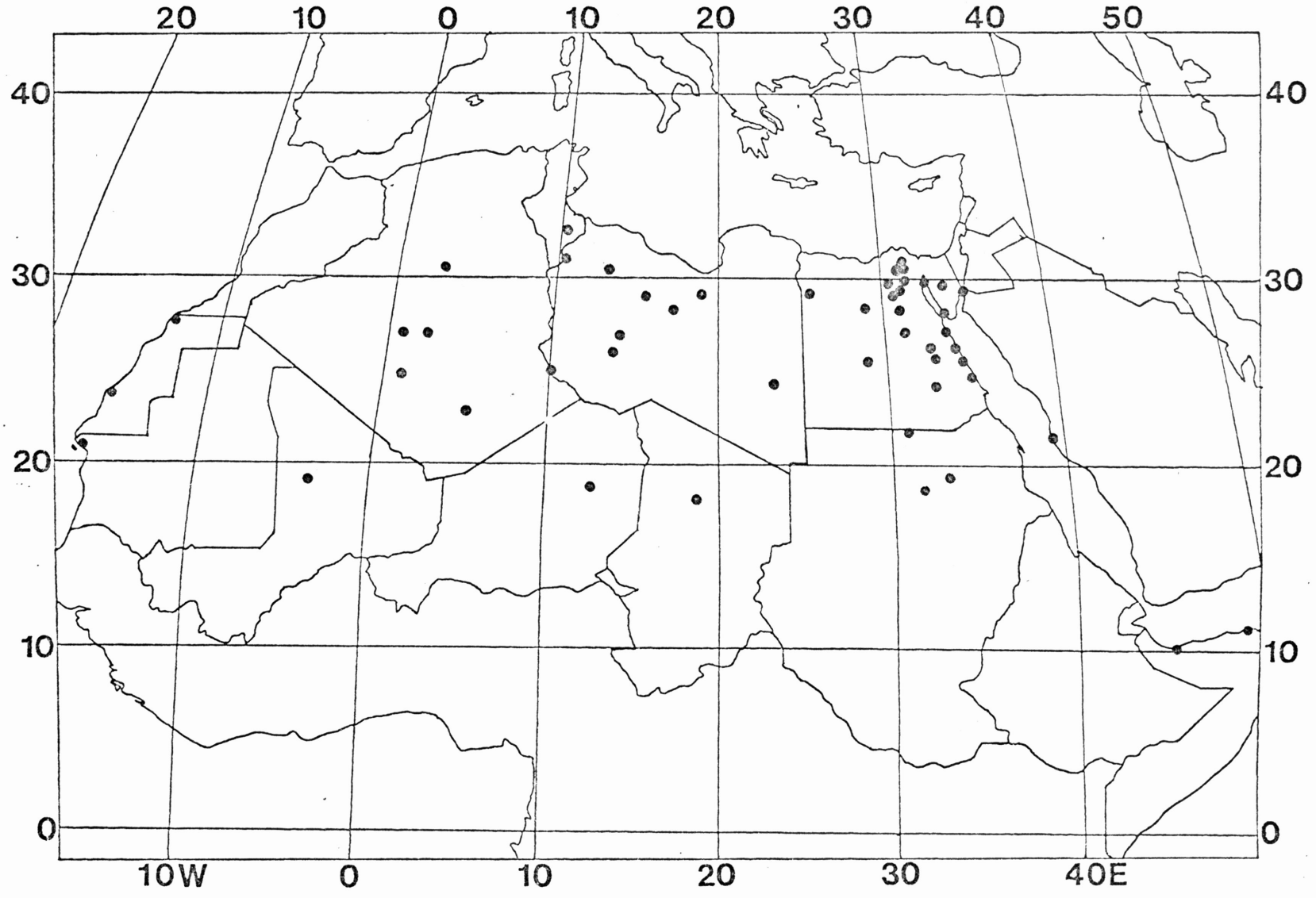

Fig. 1. Location of stations in North Africa.

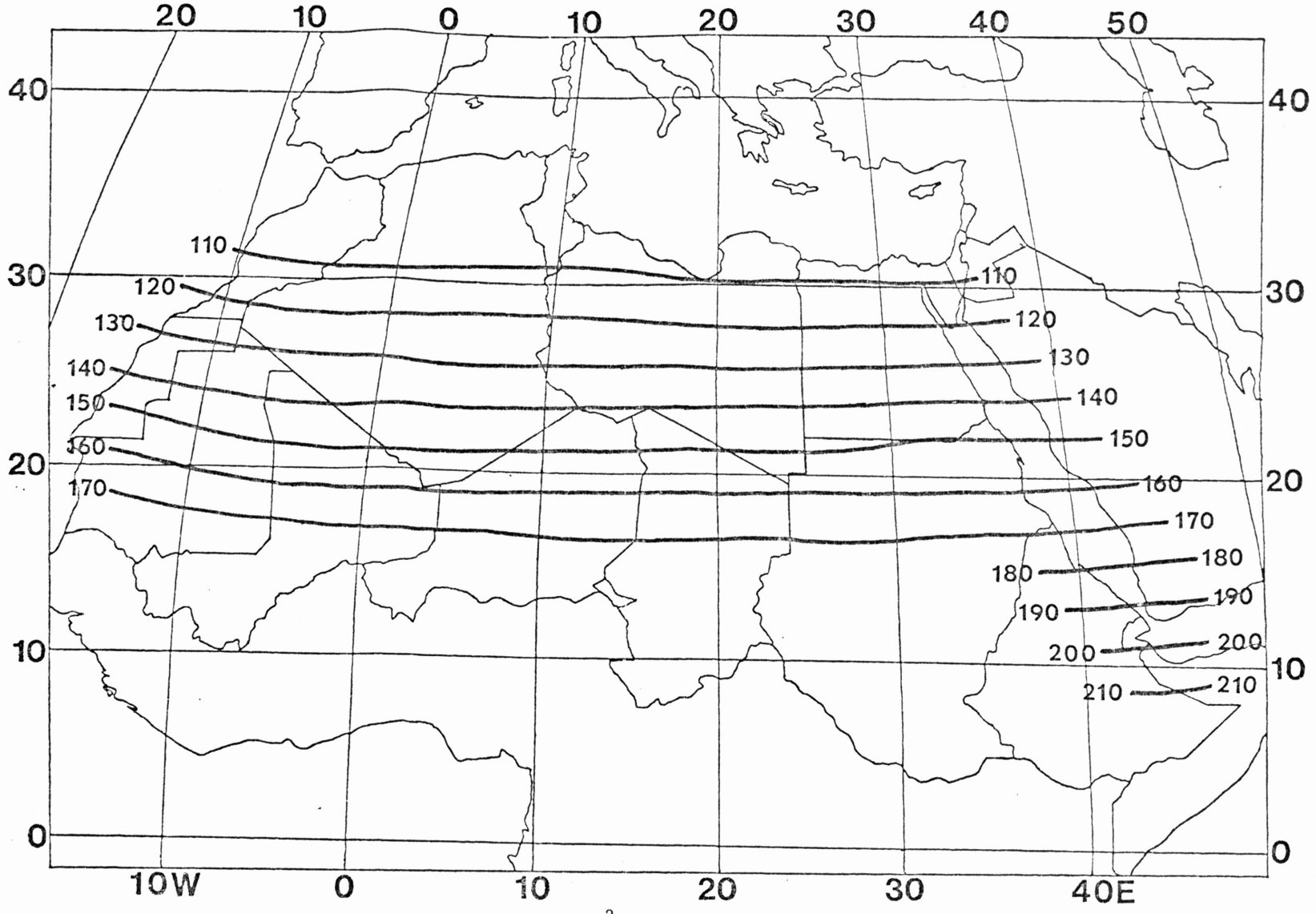

Fig. 2. Mean solar radiation absorbed (W m^{-2}) for January.

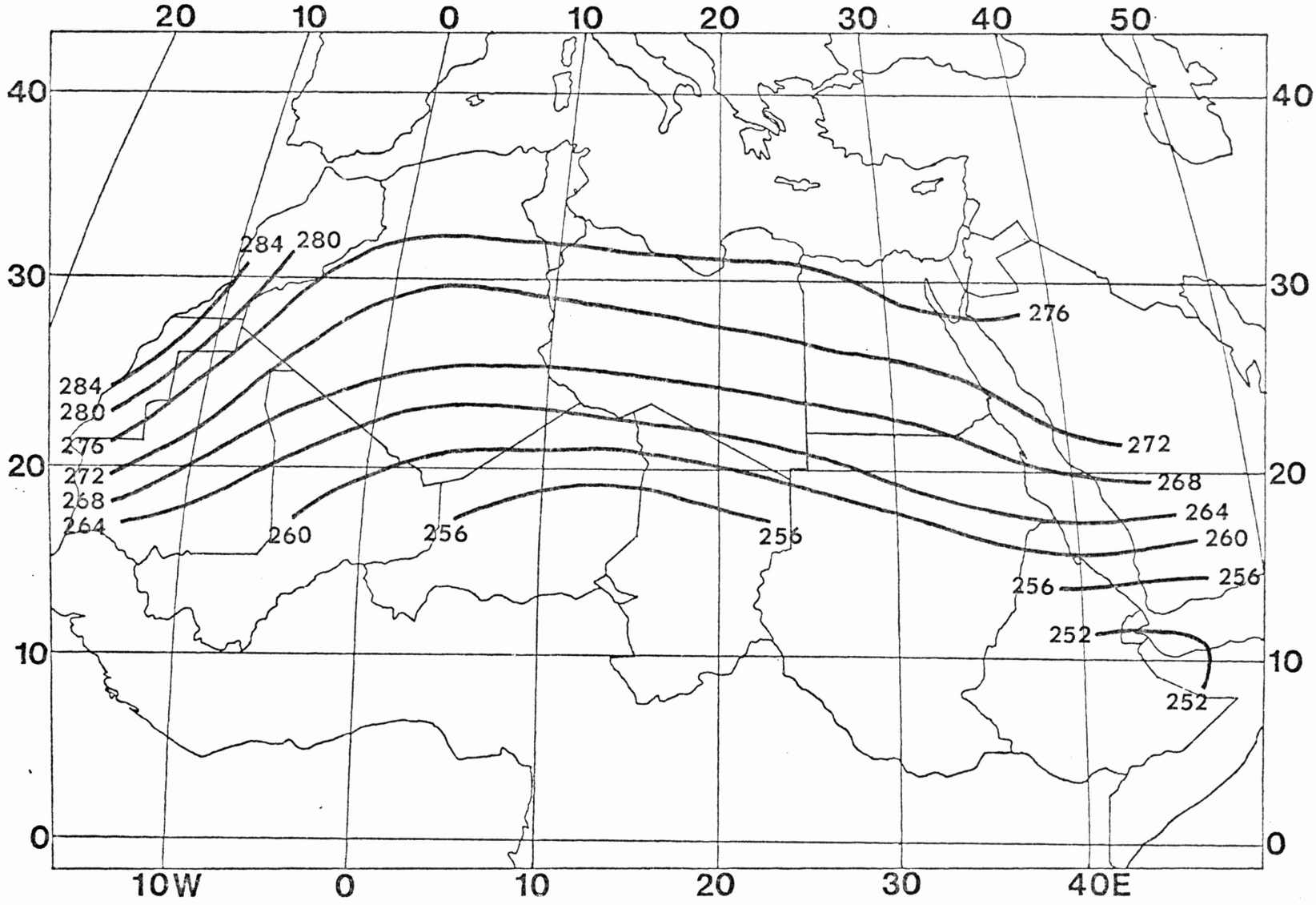

Fig. 3. Mean solar radiation absorbed (W m^{-2}) for July.

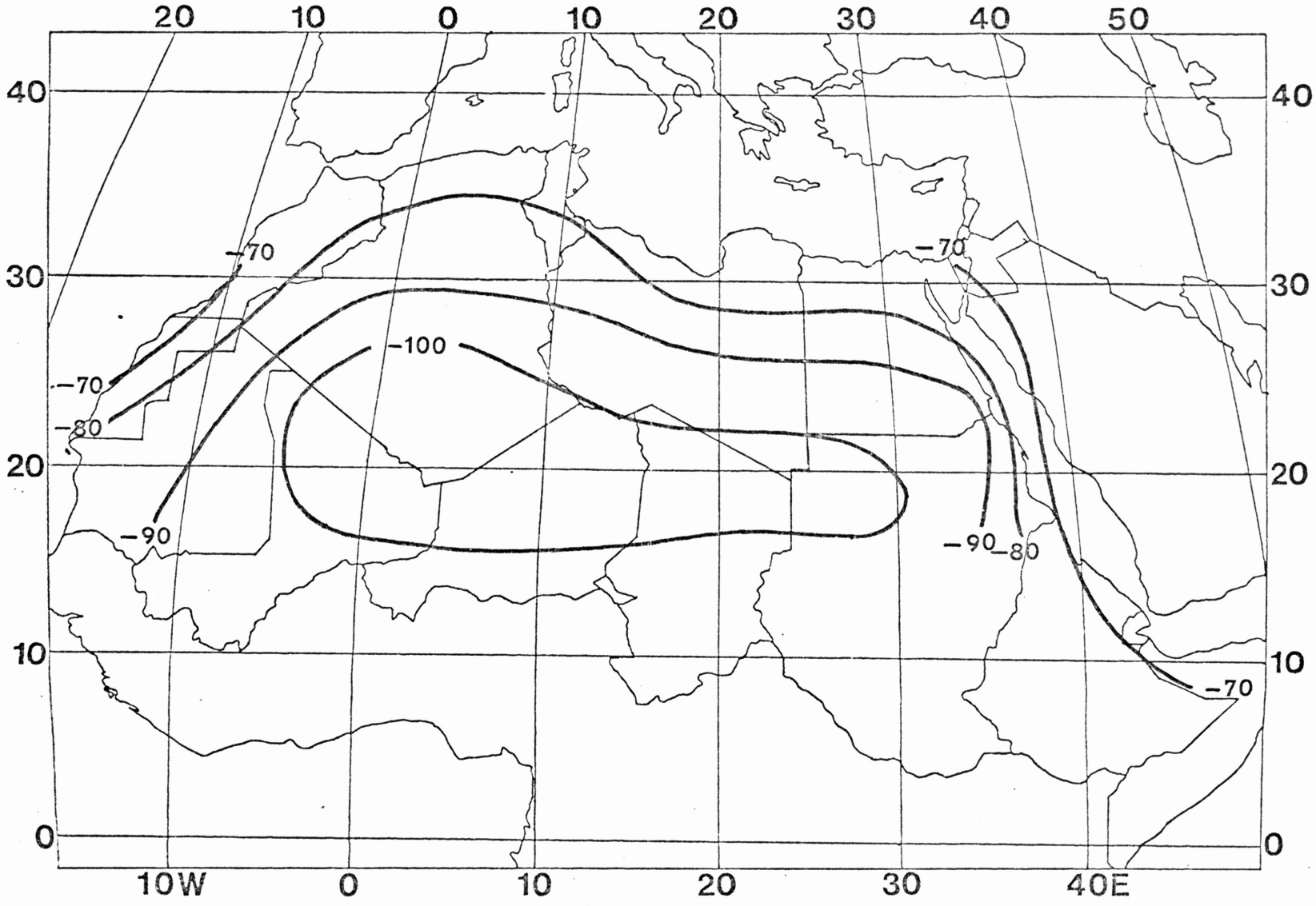

Fig. 4. Mean net longwave radiation (W m^{-2}) for January.

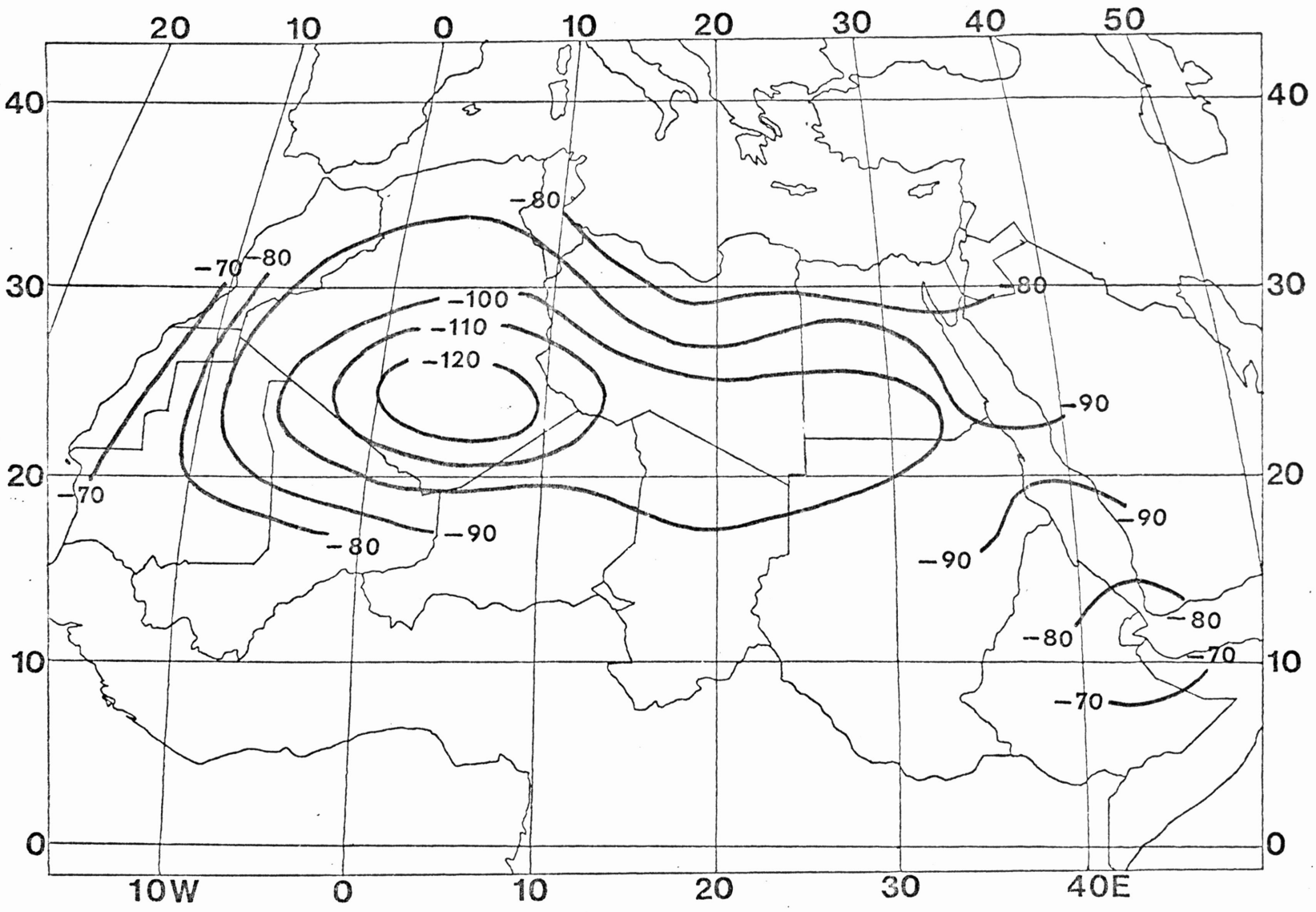

Fig. 5. Mean net longwave radiation (W m^{-2}) for July.

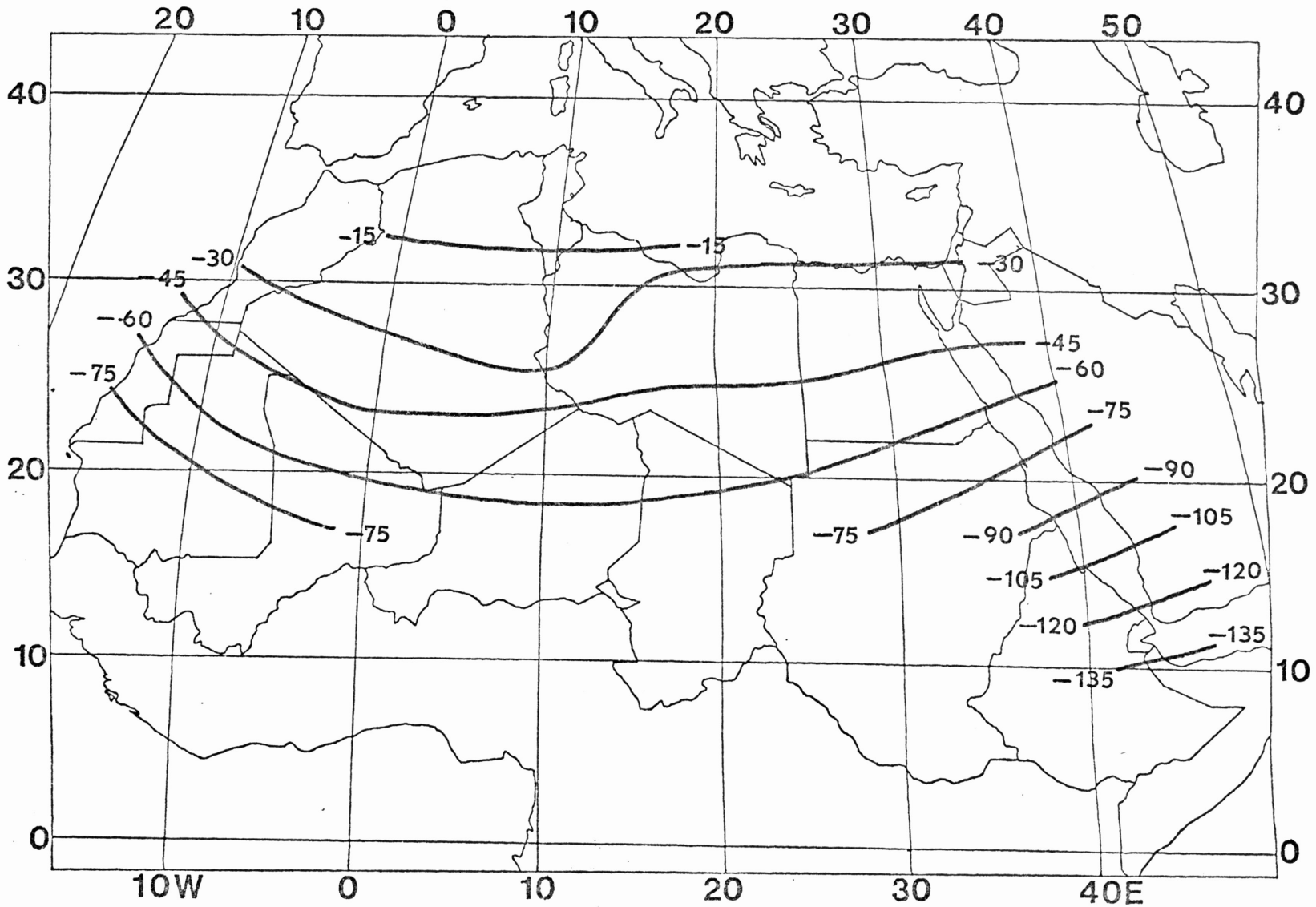

Fig. 6. Mean sensible heat flux (W m^{-2}) for January.

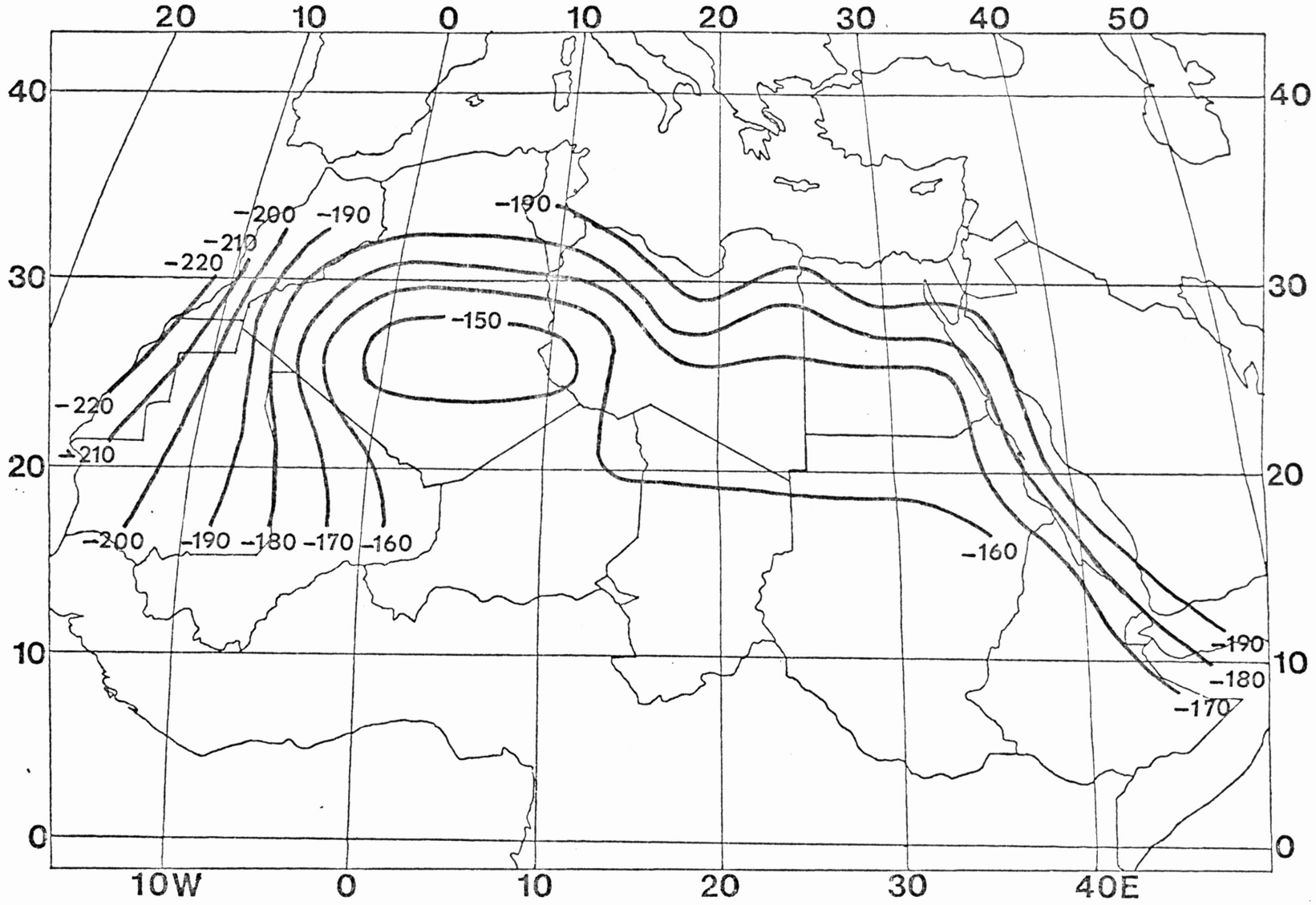

Fig. 7. Mean sensible heat flux (W m^{-2}) for July.

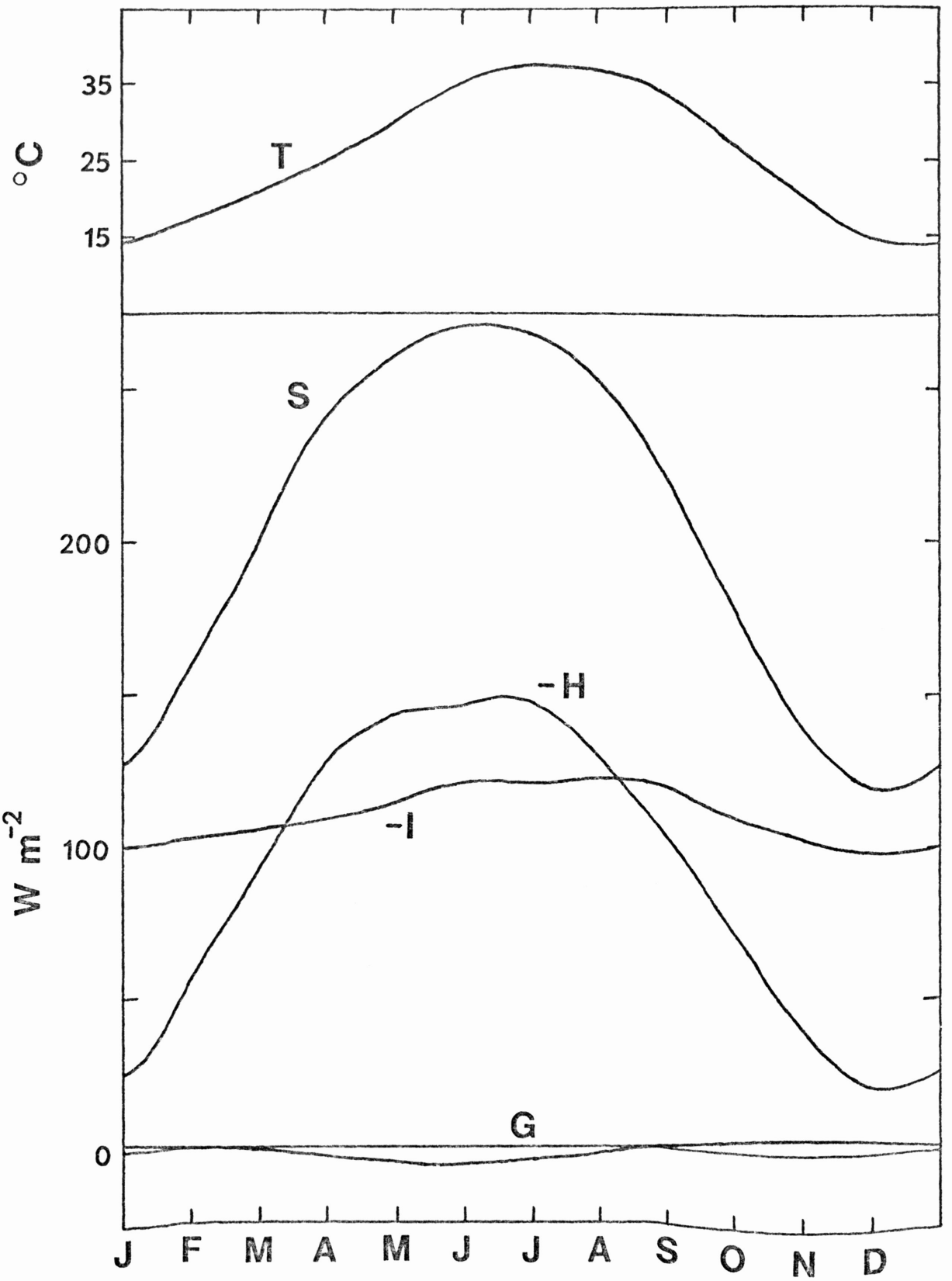

Fig. 8. Average annual variation of the air temperature and components of the surface energy balance at Aoulef, Algeria (26.97N). LE is negligible.

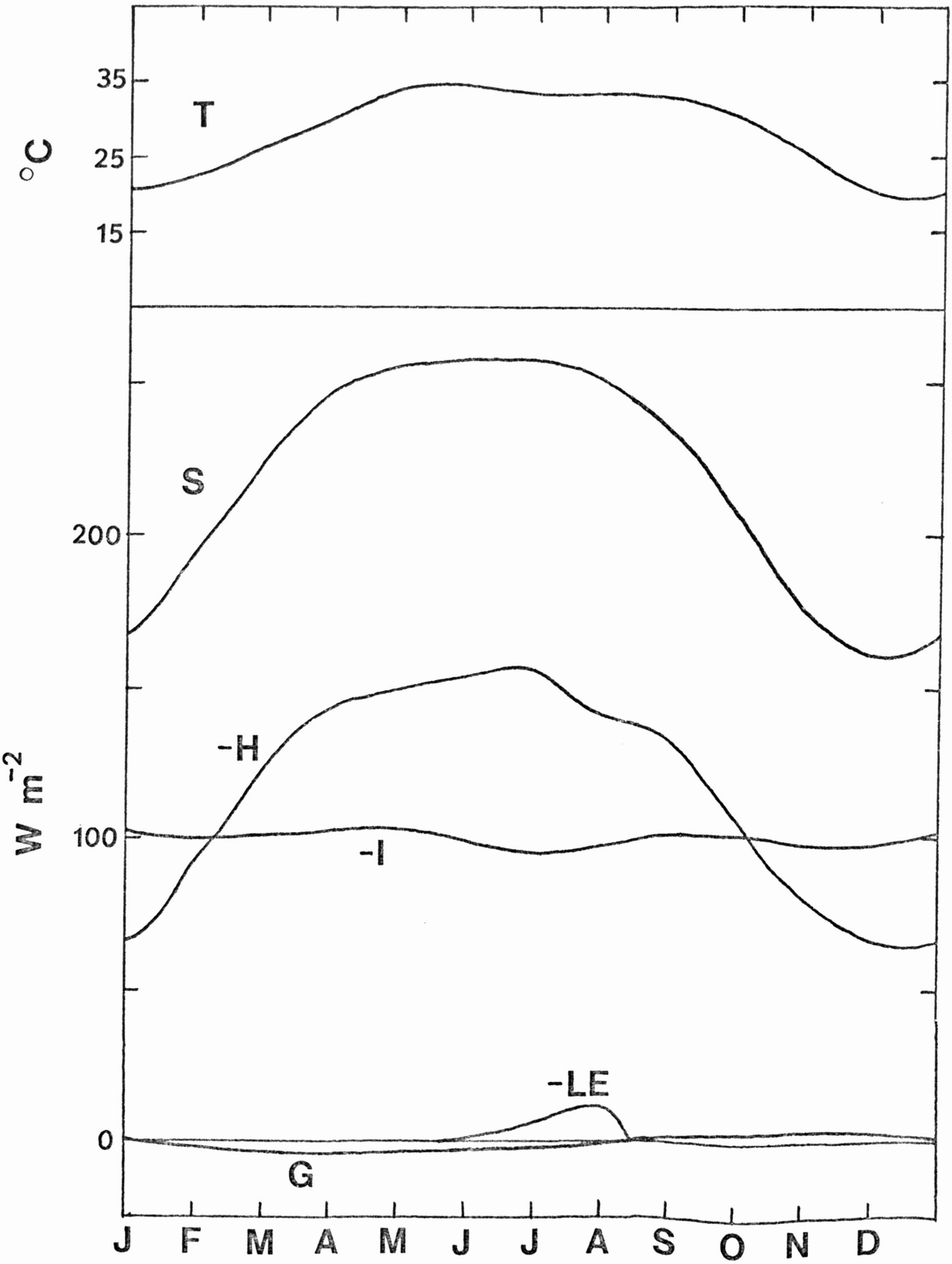

Fig. 9. Average annual variation of the air temperature and components of the surface energy balance at Faya-Largeau, Chad (18.00N).

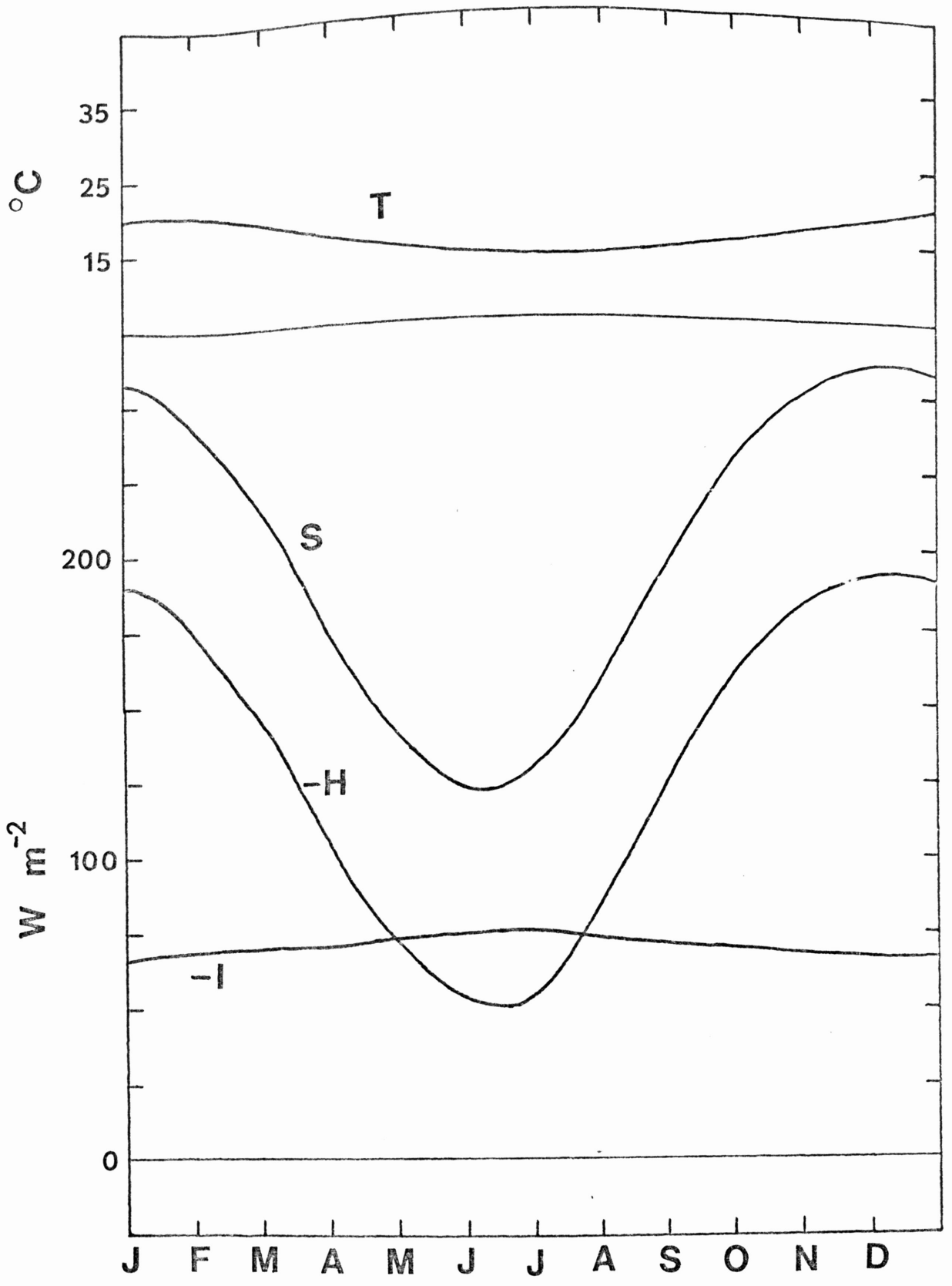

Fig. 10. Average annual variation of the air temperature and components of the surface energy balance at Antofagasta, Chile (23.47S). LE and G are negligible.

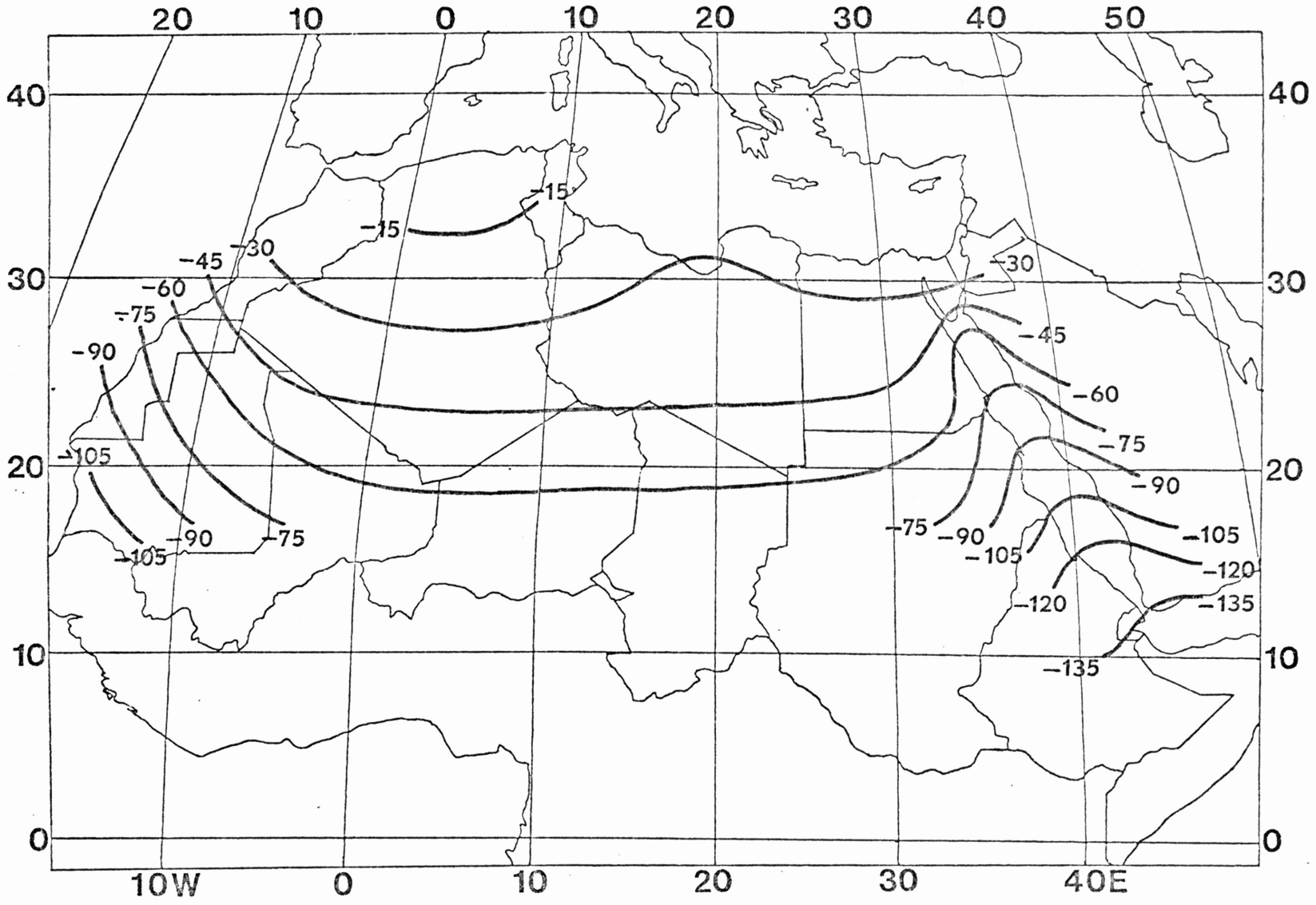

Fig. 11. Mean regression sensible heat flux (W m^{-2}) for January.

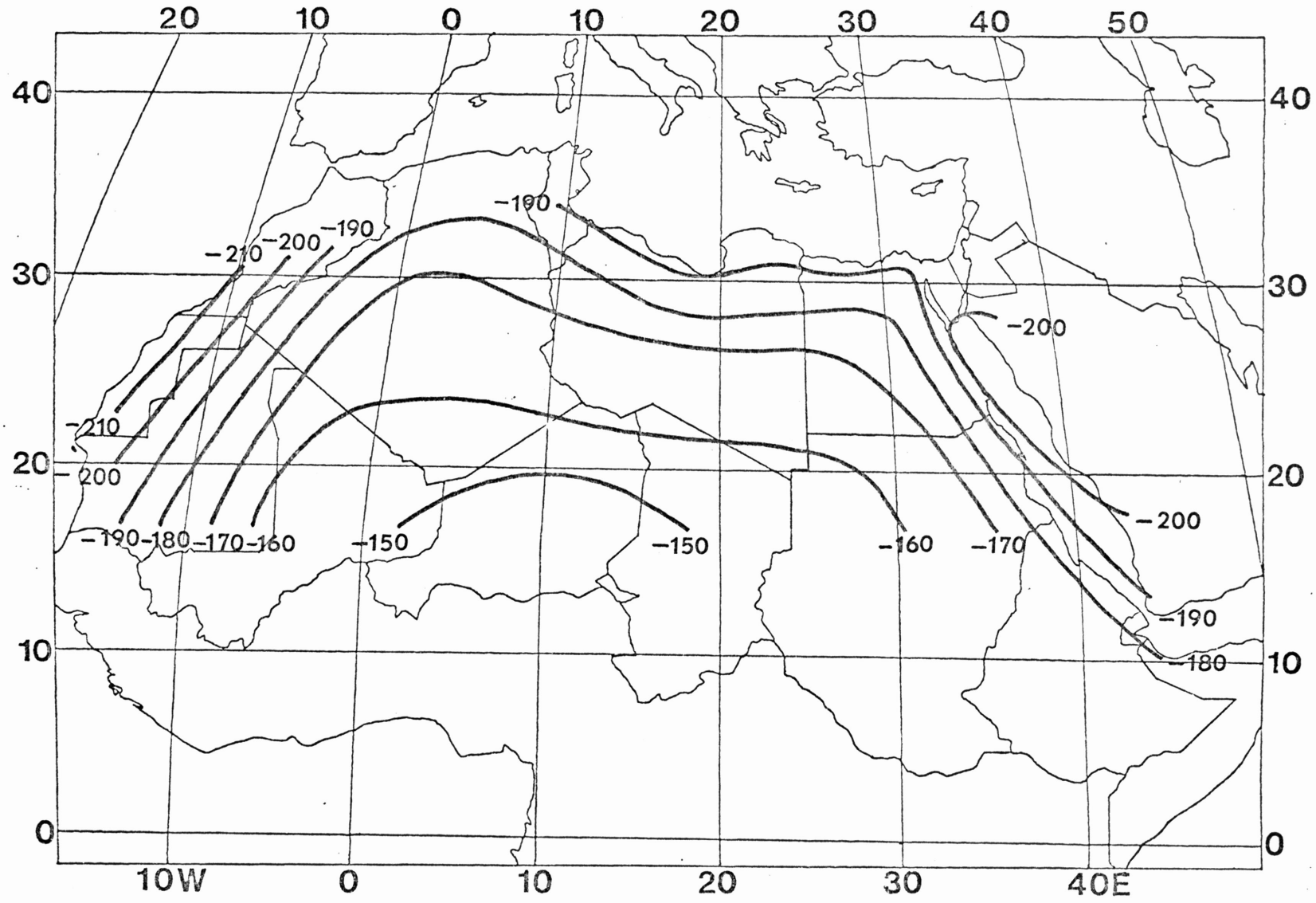

Fig. 12. Mean regression sensible heat flux (W m^{-2}) for July.

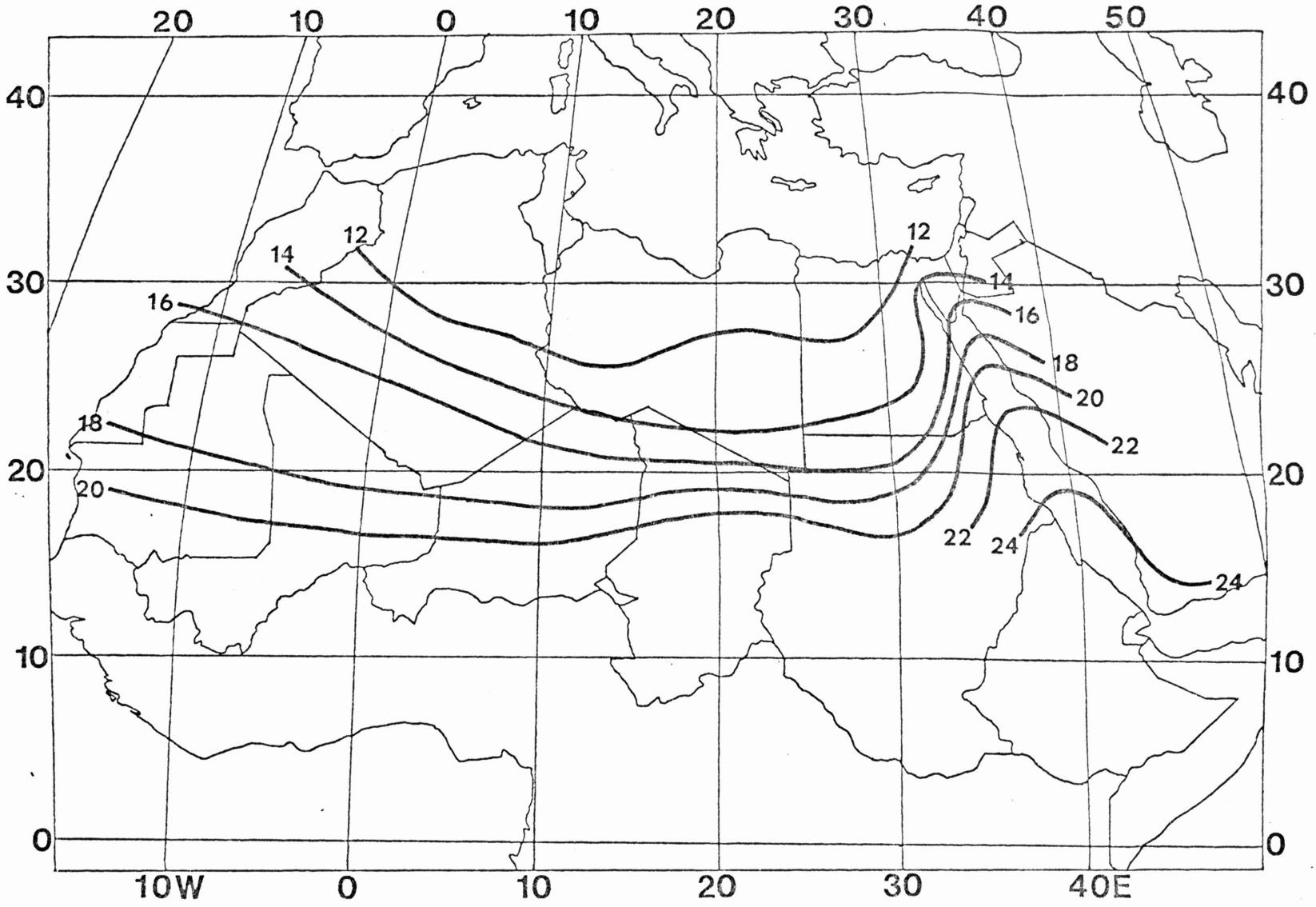

Fig. 13. Observed mean surface air temperature (°C) for January.

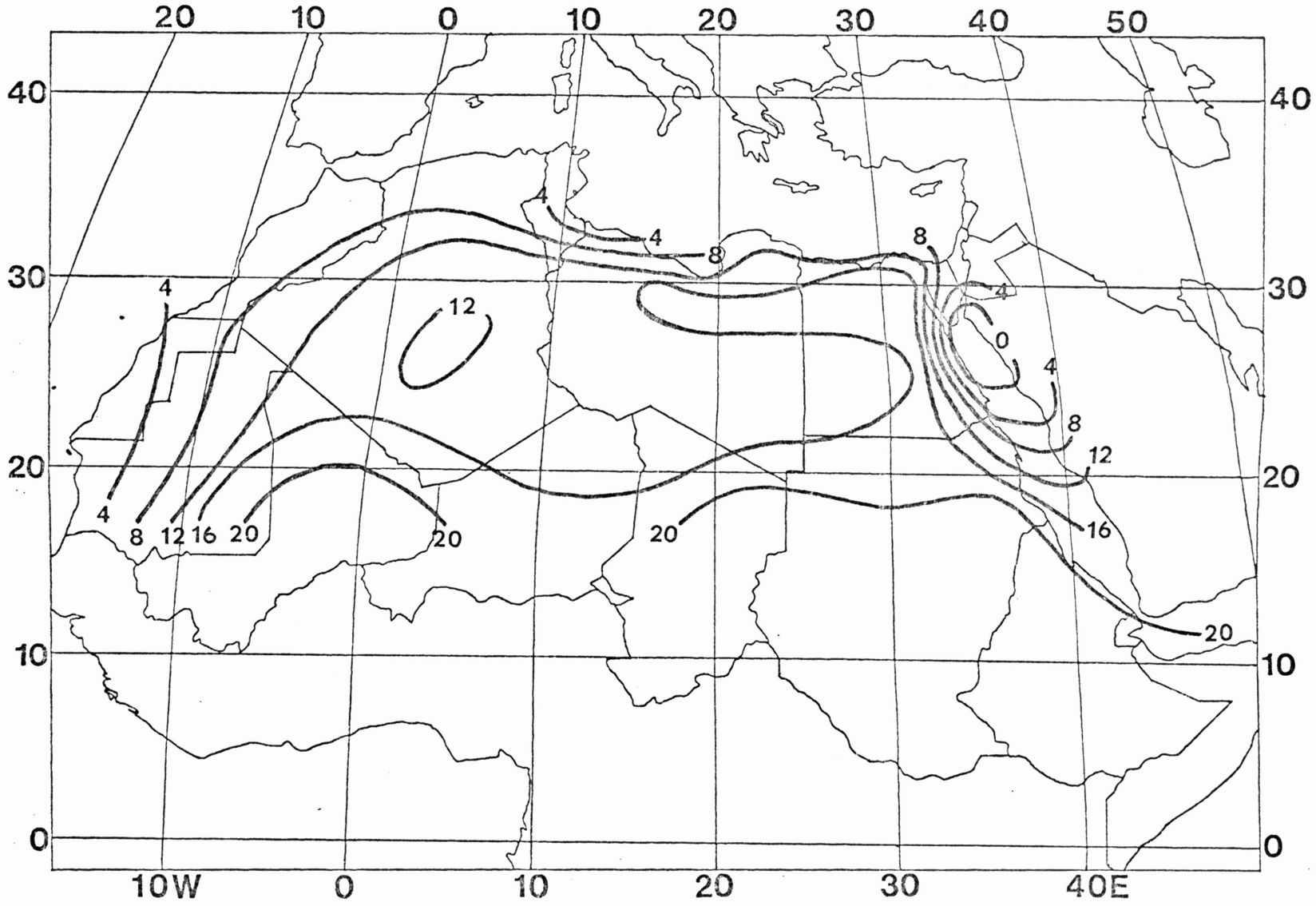

Fig. 14. Computed mean surface air temperature (°C) for January.

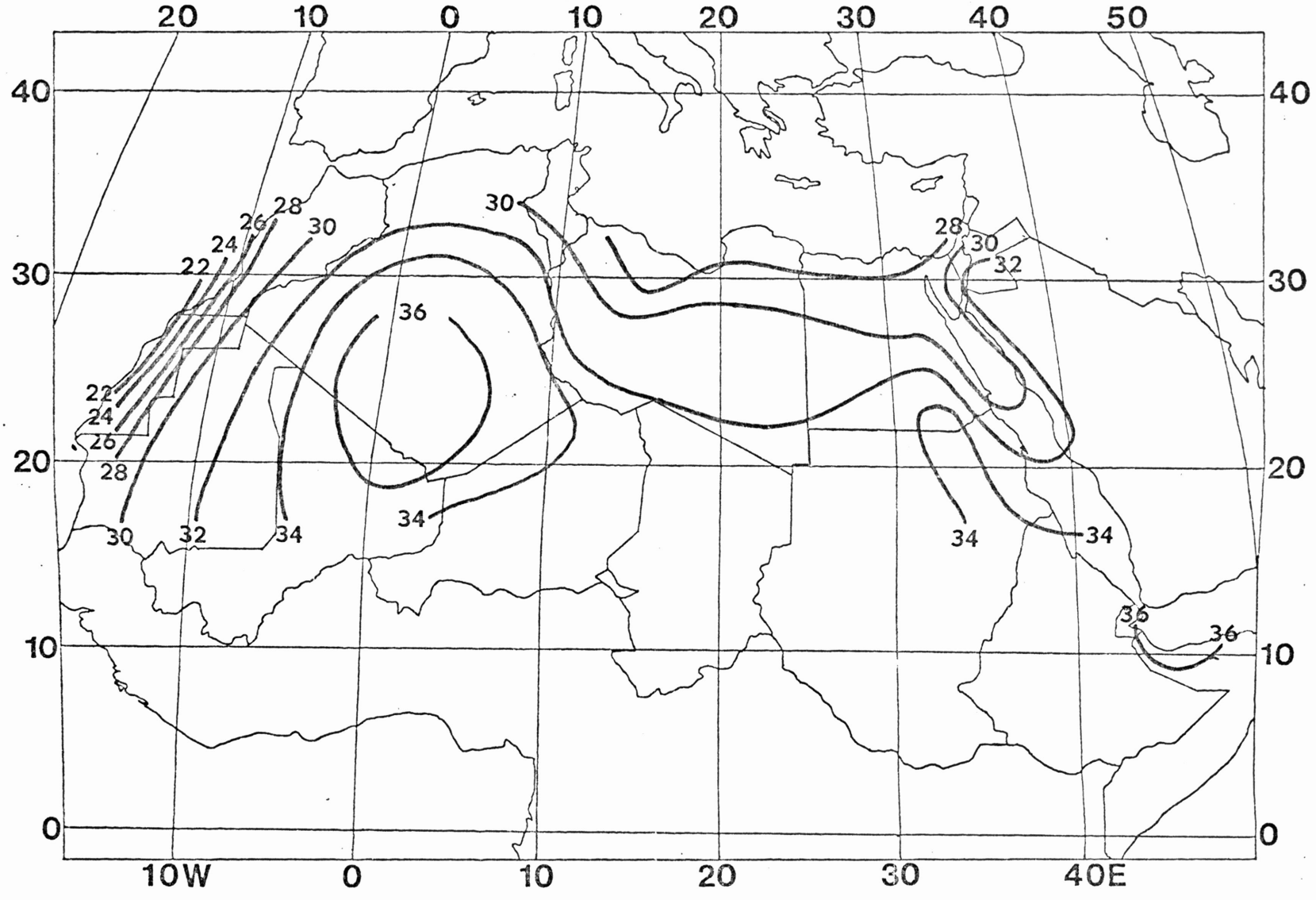

Fig. 15. Observed mean surface air temperature (°C) for July.

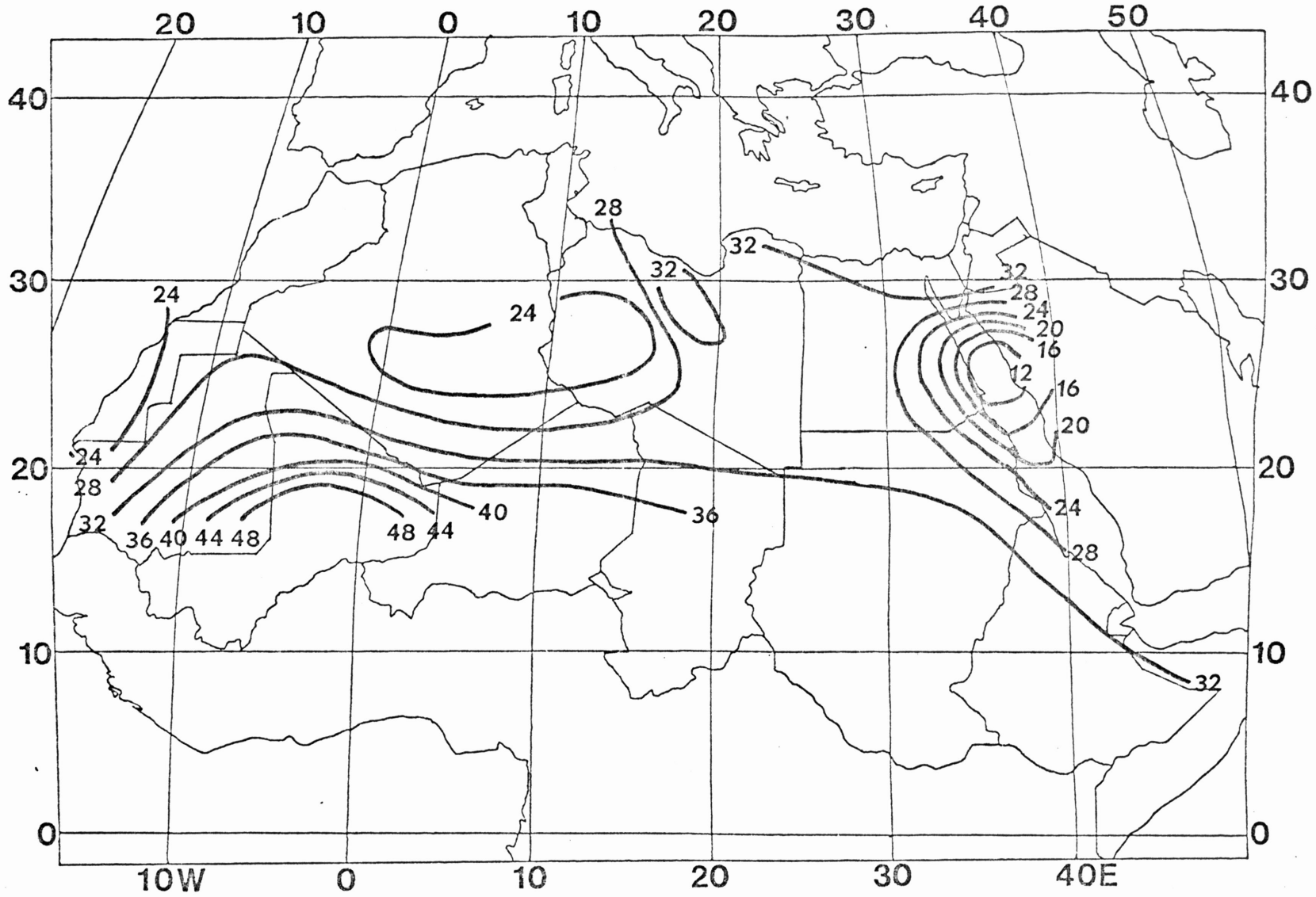

Fig. 16. Computed mean surface air temperature (°C) for July.

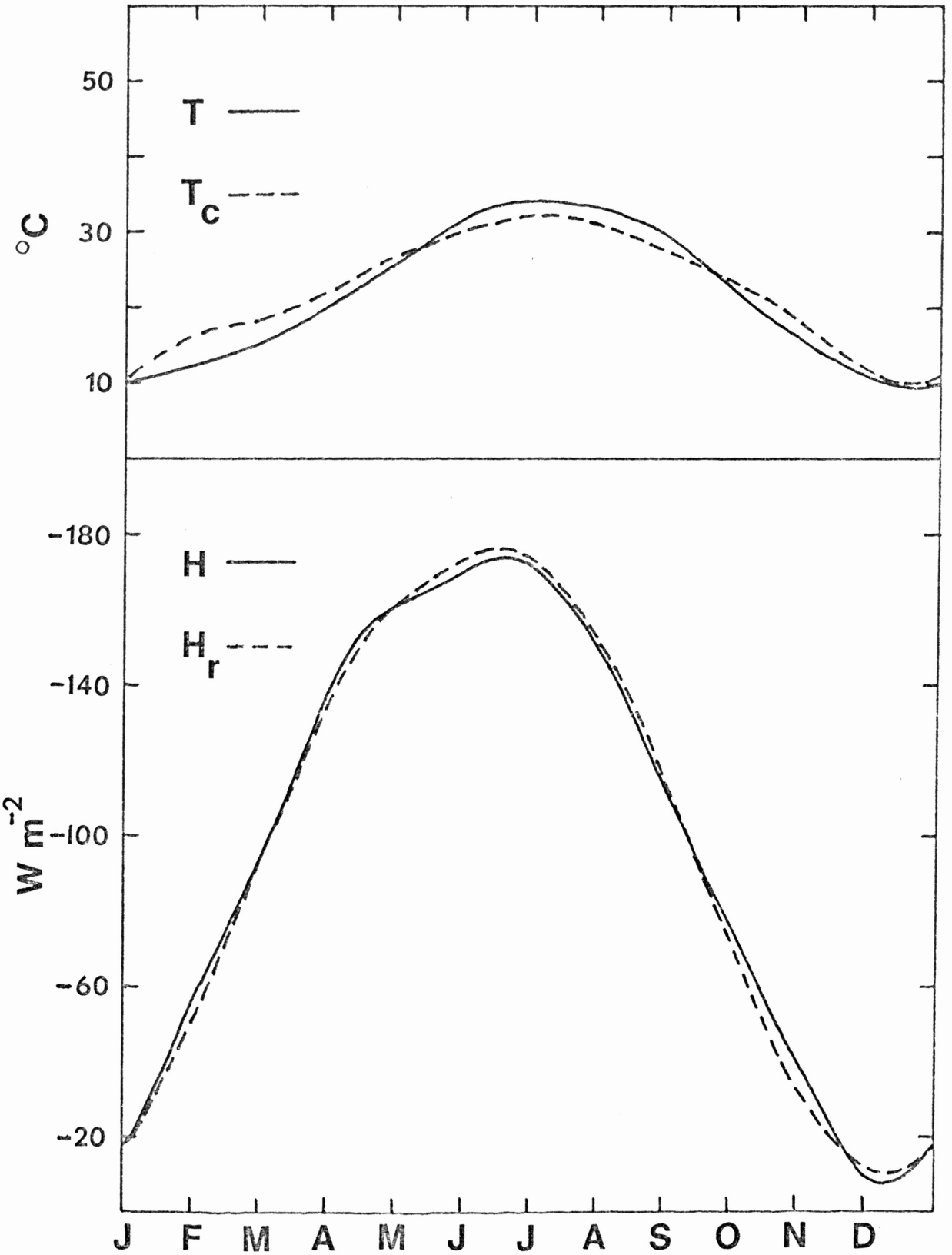

Fig. 17. Annual variation of observed temperature (T), sensible heat flux (H), computed temperature (Tc), and regression sensible heat flux (Hr) for El Golea, Algeria (30.57N).

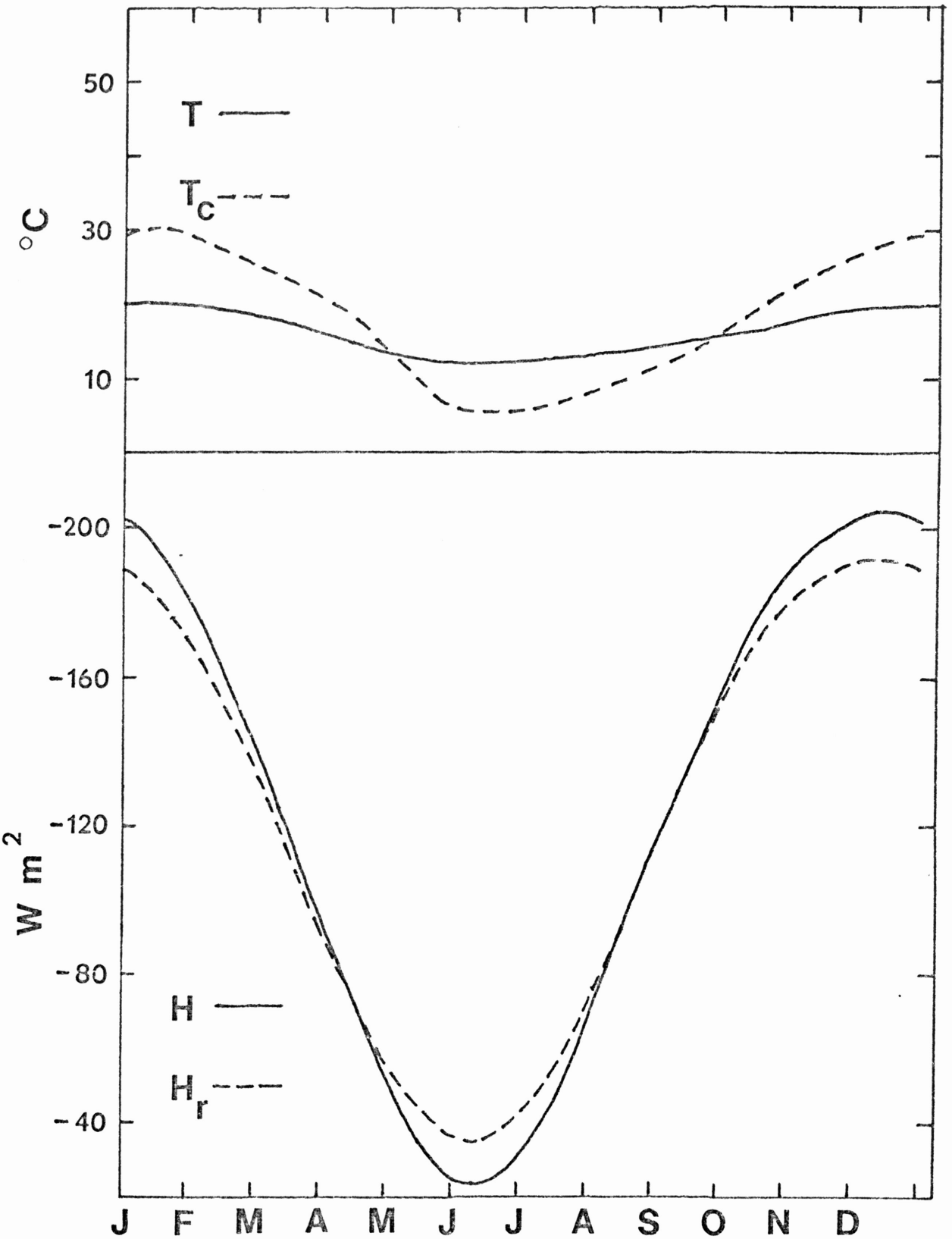

Fig. 18. Annual variation of observed temperature (T), sensible heat flux (H), computed temperature (Tc), and regression sensible heat flux (Hr) for Copiapo, Chile (27.35S).

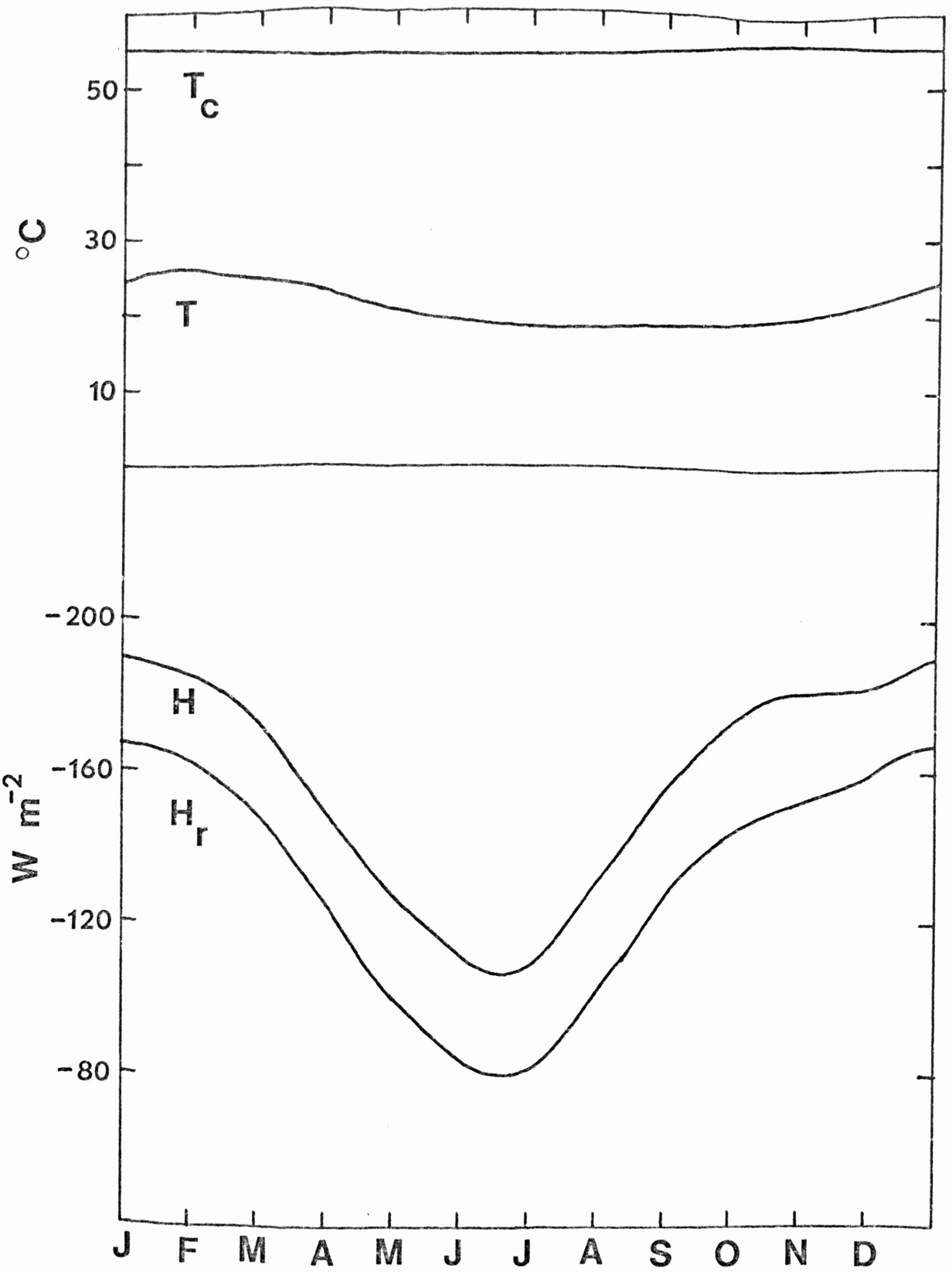

Fig. 19. Annual variation of observed temperature (T), sensible heat flux (H), computed temperature (Tc), and regression sensible heat flux (Hr) for Casa Grande, Peru (7.68S).

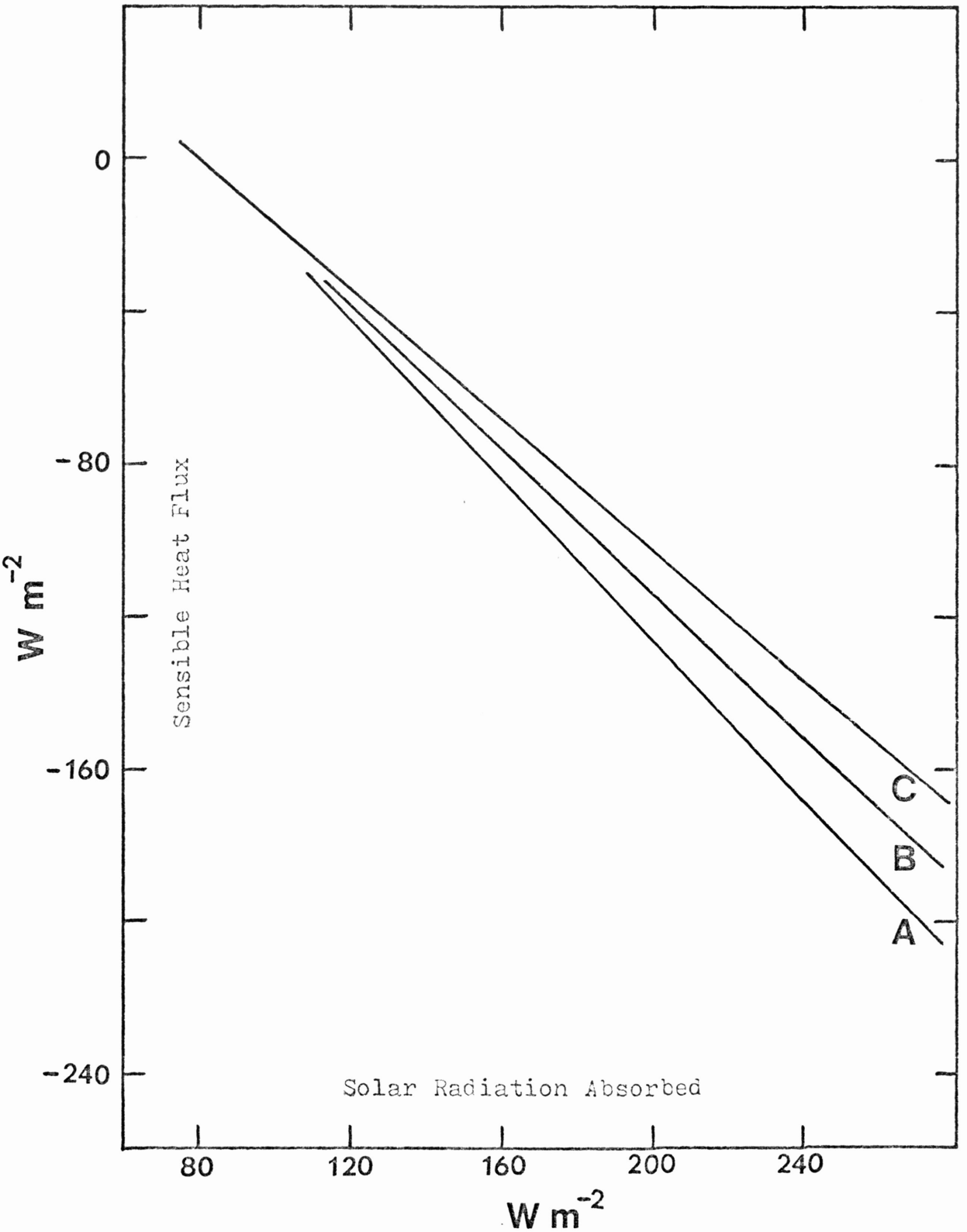

Fig. 20. Sensible heat flux as a function of solar radiation absorbed for three locations. A. Luderitz Bay, Namibia (26.63S). B. Tor, Egypt (28.23N). C. Greenland Ranch, California, United States (36.47N).

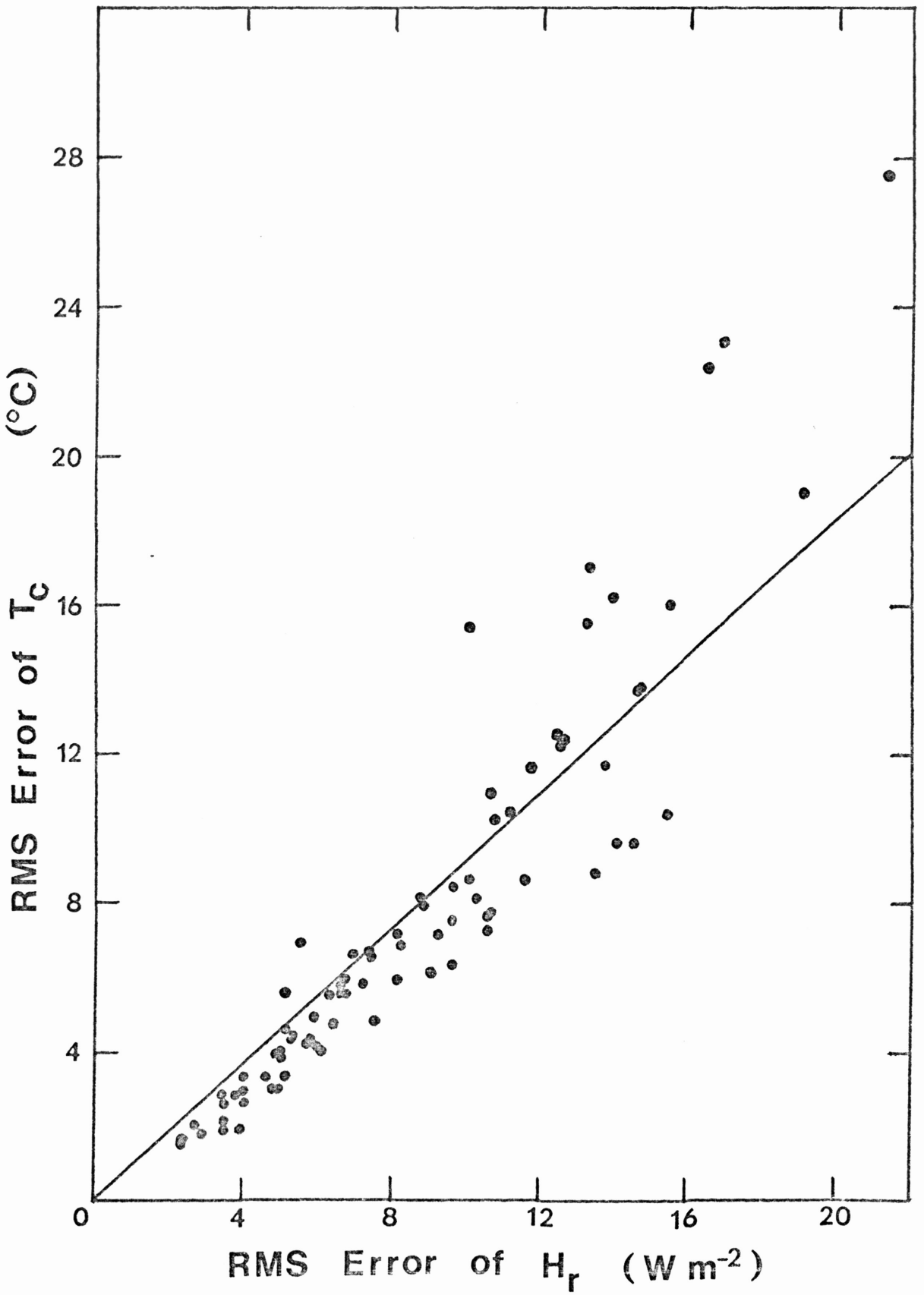

Fig. 21. RMS error of computed temperature as a function of RMS error or regression sensible heat flux.

REFERENCES

Barry, R. G., and R. J. Chorley, 1970: Atmosphere, Weather, and Climate. New York, Holt, Rinehart and Winston, Inc., 320 pp.

Berliand, M. E., and T. G. Berliand, 1952: Determination of the effective outgoing radiation of the earth, taking into account the effect of cloudiness. Izv. Akad. Nauk SSSR, Ser. Geofiz. No. 1.

Berliand, T. G., 1960: Methods for climatological computation of global radiation. Meteorol. Hydrol., No. 6.

Bhumralker, C. M., 1975: Numerical experiments on the computation of ground surface temperature in an atmospheric general circulation model. J. Appl. Meteor., 14, 1246-1258.

Bryson, R. A., Editor, 1974: World Survey of Climatology. Vol.11 , New York, Elsevier, 420 pp.

Budyko, M. I., 1963: Atlas of the Heat Balance of the Earth. Academy of Sciences, Moscow, 69 pp.

_____, 1974: Climate and Life. New York, Academic Press, 508 pp.

Griffiths, J. F., Editor, 1972: World Survey of Climatology. Vol. 10, New York, Elsevier, 604 pp.

Hammond Medallion World Atlas, 1971: Hammond, Inc., 415 pp.

Houghton, H. G., 1954: On the annual heat balance of the northern hemisphere. J. Meteor., 11, 1-9.

Jacobs, C. A., and P. S. Brown, Jr., 1973: An investigation of the numerical properties of the surface heat balance. J. Appl. Meteor., 12, 1069-1072.

Ketter, R. L., and S. P. Prawel, Jr., 1969: Modern Methods of Engineering Computation. New York, McGraw-Hill, Inc., 492 pp.

Myrup, L. O., 1969: A numerical model of the urban heat islands. J. Appl. Meteor., 8, 908-918.

Outcalt, S. I., 1972: The development and application of a simple digital surface climate simulator. J. Appl. Meteor. 11, 629-636.

Priestly, C. H. B., 1959: Heat conduction and temperature profiles in air and soil. J. Aust. Inst. Agr. Sci., 25, 94-107.

Rumney, G. R., 1968: Climatology and the World's Climates. London, The Macmillan Co., 656 pp.

Saltzman, B., 1967: On the theory of the mean temperature of the earth's surface. Tellus, 19, 219-229.

Schutz, C., and W. L. Gates, 1971: Global Climatic Data for Surface, 800mb, 400mb: January. The Rand Corporation, R-915-ARPA 173 pp.

_____, and _____, 1972a: Supplemental Global Climatic Data: January. The Rand Corporation, R-915/1-ARPA, 41 pp.

_____, and _____, 1972b: Global Climatic Data for Surface, 800mb, 400mb: July. The Rand Corporation, R-1029-ARPA, 180 pp.

_____, and _____, 1973. Supplemental Global Climatic Data: January. The Rand Corporation, R-915/2-ARPA, 38 pp.

_____, and _____, 1974: Supplemental Global Climatic Data: July. The Rand Corporation, R-1029/1-ARPA, 38 pp.

Sellers, W. D., 1965: Physical Climatology. The University of Chicago Press, 272 pp.

Smithsonian Meteorological Tables, 1966: The Smithsonian Institution, 527 pp.

Strahler, A. N., 1965: Introduction to Physical Geography. New York, John Wiley and Sons, Inc., 455 pp.

Tuller, S. E., 1968: World distribution of mean monthly and annual precipitable water. Mon. Wea. Rev., 96, 785-797.

U. S. Department of Commerce, ESSA, 1966: World Weather Records: 1951-1960. Vol. 3, Washington, D. C., 355 pp.

_____, 1967: World Weather Records: 1951-1960. Vol. 5, Washington, D. C., 545 pp.

Vernekar, A. D., 1975: A calculation of normal temperature at the earth's surface. J. Atmos. Sci., 32, 2067-2081.

Vries, D. A. de, 1958: The thermal behaviour of soils. Climatology and Microclimatology, Paris, UNESCO, 109-113.

Wernstedt, F. L., 1961a: World Climatic Data: Africa. Penn State University, Edwards Brothers, Inc..

_____, 1961b: World Climatic Data: Latin America and the Caribbean. Penn State University, Edwards Brothers, Inc..

Appendix

Eq. (2) is an expression for the instantaneous flux of solar radiation absorbed by a horizontal surface on Earth. An expression for the zenith angle of the sun can be written

$$\cos\theta = \sin\phi \sin\delta - \cos\phi \cos\delta \cos t, \tag{A1}$$

or

$$\cos\theta = A + B \cos t,$$

where ϕ is latitude, δ is the solar declination, and t is the hour angle starting at midnight, going from 0 to 2π.

The optical air mass is approximated by

$$m \approx \sec\theta = (A+B\cos t)^{-1}$$

Since δ and r do not change appreciably during a given day, we need only integrate (2) from sunrise to noon and double that value to determine the solar radiation absorbed during a full day. Thus,

$$S_i = 2(1 - \bar{\alpha})\left(\frac{r_m}{r}\right)^2 S' \int_{t_{ri}}^{t_{ni}} Q(t)\, dt \tag{A2}$$

where S_i is the total energy absorbed on a given day, and

$$Q(t) = \tau^{[(A+B\cos t)^{-1}]}(A+B\cos t),$$

t_{ri} is the hour angle of sunrise, and t_{ni} is the hour angle at noon, or π. Mean monthly planetary albedo is taken outside the integration because this derivation is directed toward an expression for mean monthly solar radiation absorbed. S' is an angular solar parameter, or the energy, received at a surface normal to the solar beam at the top of Earth's atmosphere per unit area during the time it takes Earth to rotate one radian relative to Sun. Earth takes 1.3751×10^4 sec to rotate one radian relative to Sun. S_o of 1353 W m^{-2} becomes S'

equal to 1.861×10^7 J m^{-2} radian $^{-1}$.

At sunrise, cos $\theta = 0$ so

$$0 = \sin\phi \sin\delta - \cos\phi \cos\delta \cos t_{ri}$$

$$t_{ri} = \text{Arccos}(\tan\phi \tan\delta) \qquad \text{(A3)}$$

For combinations of ϕ and δ that make (A3) undefined there is no daily sunrise or sunset.

To integrate (A2), a symmetrical integration formula is employed (See Ketter and Prawel, 1969, p. 235).

$$S_i = 2(1-\bar{\alpha})\left(\frac{r_m}{r}\right)^2 S' [4h(7Q_0 + 32Q_1 + 12Q_2 + 32Q_3 + 7Q_4)/90] \qquad \text{(A4)}$$

Here $h = (t_{ri}-t_{ni})/4$, and $Q_j = Q(t_{ri}+jh)$.

Q_0 is zero because cos $\theta = 0$ at sunrise. (A4) becomes

$$S_i = 0.08889h\ (1-\bar{\alpha})\left(\frac{r_m}{r}\right)^2 S'(32Q_1 + 12Q_2 + 32Q_3 + 7Q_4).$$

Mean monthly solar radiation absorbed is simply

$$S = \frac{1}{\Delta t} \sum_{i=1}^{N} S_i$$

where N is the number of days in the month and Δt is the length of the month.

Values of δ (radians) and r (meters) were calculated by the following formulas.

$$\delta = 0.00527 + 0.41 \cos[0.0172(x - 172.7)] + 0.0059 \cos[0.0344(x-89.1)],$$

$$r = r_m/[1 + \varepsilon\{-0.01443 + \cos[0.0172(x-3.5)] + 0.0144 \cos[0.0344 (x - 3.6)]\}]$$

where x is the day of the year,

ε is the eccentricity of Earth's orbit, equal to 0.0167, and

$r_m = 1.495 \times 10^{11}$ meters.